EXCITON CONDENSATE DRIVEN FORCE IN DOUBLE LAYER SYSTEMS

A DISSERTATION SUBMITTED TO
THE GRADUATE SCHOOL OF ENGINEERING AND SCIENCE
OF BILKENT UNIVERSITY
IN PARTIAL FULFILLMENT OF THE REQUIREMENTS FOR
THE DEGREE OF
DOCTOR OF PHILOSOPHY
IN
PHYSICS

By
Ege Özgün
February, 2016

EXCITON CONDENSATE DRIVEN FORCE IN DOUBLE LAYER SYSTEMS

By Ege Özgün

February, 2016

We certify that we have read this dissertation and that in our opinion it is fully adequate, in scope and in quality, as a dissertation for the degree of Doctor of Philosophy.

Tuğrul Hakioğlu(Advisor)

Ceyhun Bulutay

Afif Sıddıki

Balazs Hetényi

Levent Subaşı

Approved for the Graduate School of Engineering and Science:

Levent Onural
Director of the Graduate School

ABSTRACT

EXCITON CONDENSATE DRIVEN FORCE IN DOUBLE LAYER SYSTEMS

Ege Özgün
Ph.D. in Physics
Advisor: Tuğrul Hakioğlu
February, 2016

Excitonic systems are challenging to deal with both theoretically and experimentally but in return, they offer a very rich physics and exotic features. We will investigate their properties under weak magnetic field and the resultant instabilities reminiscent of Sarma-I and Sarma-II phases. A new type of force in condensed matter physics, emerging due to the presence of the excitonic condensation will be demonstrated via semi-analytical and numerical calculations in two different systems of GaAs double quantum well geometries and layered transition metal dichalcogenide material $1T\text{-}TiSe_2$. Competition of charge-density wave and exciton condensate orders in layered systems will also be discussed in detail and an alternative explanation for the periodic lattice distortions observed in $1T\text{-}TiSe_2$ will be posed.

Keywords: Exciton condensation, charge-density waves, double quantum wells.

ÖZET

ÇİFT KATMANLI SİSTEMLERDE EGZİTON YOĞUŞMASINDAN DOĞAN KUVVET

Ege Özgün
Fizik, Doktora
Tez Danışmanı: Tuğrul Hakioğlu
Şubat, 2016

Egzitonik sistemler, hem deneysel hem de teorik olarak zorlayıcı sistemlerdir ama bunun karşılığında oldukça zengin bir fizik ve egzotik özellikler sunarlar. Bu sistemlerin zayıf manyetik alan altındaki özelliklerini ve ortaya çıkan, Sarma-I ve Sarma-I benzeri kararsızlıkları inceleyeceğiz. Egziton yoğuşmasının varlığında ortaya çıkan, yoğun madde fiziğindeki yeni bir tip kuvveti, nümerik ve yarı analitik metotlar ile, biri GaAs çift kuvantum kuyusu geometrisi, diğeri ise katmanlı geçiş metali dikalkojenlerinden $1T$-$TiSe_2$ olan iki farklı sistemde göstereceğiz. Yük yoğunluğu dalgaları ve egziton yoğuşması düzenlerinin mücadelesini ve $1T$-$TiSe_2$ malzemesinde gözlemlenmiş olan periodik sapmalar için alternatif bir senaryoyu da detaylı bir biçimde inceleyeceğiz.

Anahtar sözcükler: Egziton yoğuşması, yük yoğunluğu dalgaları, çift kuvantum kuyuları.

Acknowledgement

I would like to thank my supervisor Prof. Tuğrul Hakioğlu for his supports and for his excellent supervising which has significantly increased my understanding of physics and science. I thank my family for their never-ending support. And finally and most importantly, I would like to thank my love, meaning of my life, Pelin Tören for motivating me in completing my thesis and making my life wonderful.

Contents

List of Figures

Chapter 1

Introduction

Excitons are composite bosons created by the electron-hole bound state in the semiconductor background. In 1924 S.N. Bose and A. Einstein represented a new phase of matter, the well-known Bose-Einstein condensation[1, 2], in which under a critical temperature bosons start to condense in the ground state. It was first Moskalenko, Blatt, Ber and W. Brandt to theoretically suggest in 1960s the Bose-Einstein condensation of a dilute exciton gas[3, 4] also referred as exciton condensation. We will deal with the many body low temperature collective effects in excitonic systems. In particular, dilute exciton gas should Bose-Einstein condense at a much higher critical temperature than atomic boson gases, thanks to higher spin degeneracy and lower effective mass. These properties of the exciton gas under sufficiently low temperatures makes the problem still a hot research topic today. The experiments on the condensed state was inconclusive until recently. The modern exciton experiments are performed using coupled quantum wells [5, 6, 7, 8] which supplies a factor of 1000-10000 enhancement in exciton lifetime compared to the former experiments that were taking place in bulk systems. Despite the advantage in the use of coupled quantum wells, the early experiments have not been totally indicative of a condensed state, leaving room for other explanations. The basic reason for this lack of evidence is that, all experiments are based on photoluminescence techniques, therefore only those exciton states that couple to light (the so called bright excitons) can be probed. Recently it is

demonstrated that dark excitons dominate the condensed ground state[9] which cannot be probed by light.

Acknowledging the categorization suggested by Snoke[10], we can present the earlier exciton condensation research under 4 main titles: a) 2D excitons in coupled quantum wells b) Coulomb drag experiments in coupled two-dimensional electron gases c) Three-dimensional excitons in the bulk semiconductor Cu_2O d) Polaritons in semiconductor microcavities. In addition to this categorization, excitons created in different semiconductor quantum wells can be formed by electron-hole pairs within the same band (both conduction or both valence) or in different bands. In the former case, the excitonic subsystem respects the particle-hole symmetry, whereas in the latter this symmetry is absent (due to different band masses as well as orbital and spin properties). Fundamental symmetry considerations in the absence of the particle-hole symmetry and their consequences have been studied recently [11, 12]. Experiments in the former case are more common (such as those by Snoke in Ref.[10].) On the other hand, the experiments carried out mostly by the Eisenstein group in Caltech[13, 14, 15, 16, 17] that respected the particle-hole symmetry, was enabled by the use of a strong magnetic field, forcing the electrons and holes to share the same type of Landau bands in different wells. Many of the experimental results performed by the Eisenstein and his colleagues have not yet been completely understood , among which are the Hall drag quantization, the presence of a sharp critical layer separation, zero bias tunneling, topological phases, superfluidity etc. In addition to these unsolved problems, it has been recently suggested that a new type of force may be present at the phase boundary (the boundary separating the condensed state from the normal exciton gas) reducing its strength (but never to zero) deep inside the condensed state[9, 18].

The longly sought evidence for the condensed state came recently by the observation of the interference fringes arising from the excitonic condensate's macroscopic wavefunction[19].

Our main interest is to device alternative and satisfactory theoretical methods for conclusive observation of the excitonic condensed state in coupled quantum

wells. In particular, we will be investigating the effect of the weak magnetic fields on the condensed state, predicting the magnitude of this new force both numerically and semi-analytically.

In Chapter 2, we will lay the basics of the excitonic systems and device the tools to handle them. Chapter 3 is devoted to the effects of a weak magnetic field on the excitonic condensate. In Chapter 4, we will start investigating the new force arising in the excitonic systems i.e. exciton condensate force (EC-force). Chapter 5 deals with the exciton condensate force and charge-density wave instability/exciton condensation competition in layered transition metal dichalcogenide material $1T\text{-}TiSe_2$. We will conclude with Chapter 6.

Chapter 2

Excitons in a nutshell

2.1 Basics of exciton physics

2.1.1 Definition of an exciton

An exciton is similar to a hydrogen atom, in which the proton is replaced by a hole i.e., excitons are bound states of electron-hole pairs. There are two different types of excitons; Frenkel excitons[20] and Wannier-Mott excitons[21, 22]. The difference between these two types of excitons is in the attraction holding them together. Since the magnitude of the attraction determines the separation between the electrons and holes, these two types will also acquire different exciton Bohr radius a_B values. Exciton Bohr radius is defined in a similar manner to the Bohr radius for the Hydrogen atom. We can follow the standard procedure to derive an expression for a_B. First we equate the Coulomb force to the rotational force:

$$\frac{e^2}{4\pi\epsilon r^2} = m_e^* \omega^2 r \tag{2.1}$$

where e, ϵ, r, m_e^* and ω are electric charge, relative permitivity, distance between

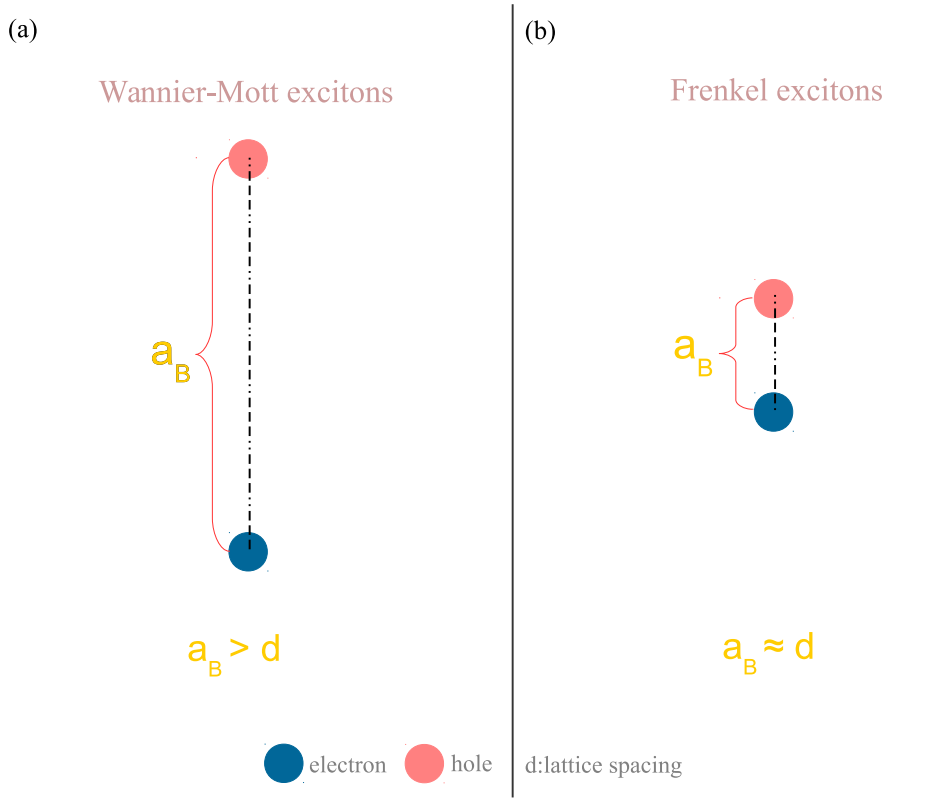

Figure 2.1: Simple illustration of Wannier-Mott and Frenkel excitons. a) Wannier-Mott excitons extend to several lattice sites with a weaker attraction between the bound electron-hole pairs. b) Frenkel excitons are tightly bound and are limited to a single lattice site.

the electron and the hole, effective electron mass and angular frequency of the electron respectively. We can recast this equation by substituting $\omega = v/r$ where v is the velocity and multiplying both sides by mr and using the Bohr-Sommerfeld quantization condition $L = n\hbar$, we have:

$$r = \frac{4\pi\epsilon\hbar^2}{m_e^* e^2} n^2 \tag{2.2}$$

Finally, setting $n = 1$ for the state with the lowest energy, i.e., ground state, we obtain the expression for the exciton Bohr radius:

$$a_B = \frac{4\pi\epsilon\hbar^2}{m_e^* e^2} \tag{2.3}$$

Let us now return to the discussion of Frenkel and Wannier-Mott excitons. Frenkel excitons are tightly bound electron-hole pairs with exciton Bohr radii

of the order of a single lattice spacing, whereas Wannier-Mott excitons are their loosely bound counterparts with exciton Bohr radius values acquiring several lattice spacings. Different types of materials give rise to different types of a_B values, since different materials have different dielectric constants and different effective band masses. We will investigate these different cases in detail in the following chapters.

It is important to define the notion of composite bosons while tackling with the excitonic systems. Electrons and holes are both fermions; by the simple angular momentum addition rules it is known that two fermions adds upto a boson. In the language of group theory, it is cast as follows:

$$\frac{1}{2} \otimes \frac{1}{2} = 0 \oplus 1 \tag{2.4}$$

The detailed explanation of angular momentum summation rules within the context of group theory can be found in Ref. [23] for instance. So excitons, which are bound states of electron-hole pairs, can be treated as composite bosons under certain conditions. We basically need to consider two quantities to determine whether our excitons can be treated as composite bosons or not: a) the exciton density $n^{(+)}$ b) the exciton Bohr radius a_B. The limiting condition comes from the commutation relation of the exciton operators[24]:

$$[c_{\mathbf{k},\sigma}, c^{\dagger}_{\mathbf{k}',\sigma'}] = \delta_{\mathbf{k},\mathbf{k}'}\delta_{\sigma,\sigma'} + \mathcal{O}(n^{(+)}a_B^3) \tag{2.5}$$

where $c_{\mathbf{k},\sigma}/c^{\dagger}_{\mathbf{k},\sigma}$ are bosonic exciton annihilation/creation operators built from the multiplication of two fermionic operators, $\mathbf{k}$ is the wavevector, σ is the spin index, and δ denotes the Kronecker delta. The above equation is a valid bosonic commutation relation if $n^{(+)}a_B^3 \ll 1$. This relation is generalized to d-dimensions by using the d-dimensional exciton density and a_B^d. Throughout this thesis, we will focus on the two-dimensional case. Recasting the above condition in 2D we have:

$$n^{(+)}a_B^2 \ll 1 \tag{2.6}$$

We will consider two different cases of $n^{(+)} \sim 10^{14}\ cm^{-2}$, $a_B = 5\mathring{A}$ and $n^{(+)} \sim 10^{11} - 10^{12}\ cm^{-2}$, $a_B = 100\mathring{A}$ which are both within the composite boson limit.

2.1.2 Electron and Hole Bands

Electrons and holes acquire effective band masses, when they are in semiconductors. There exist three main bands: electron band (conduction), light hole band (valence) and heavy hole band (valence). We will mostly deal with GaAs double quantum well (DQW) semiconductors. In these III-V semiconductors of GaAs, the typical effective masses for the aformentioned bands are given as:

$$m_e^* = 0.067m_0 \qquad m_{hh}^* = 0.45m_0 \qquad m_{lh}^* = 0.082m_0 \tag{2.7}$$

with m_0 being the electron mass in vacuum and subindices e, hh, lh denoting electron, heavy hole, light hole respectively. A simple illustration of these bands in GaAs with a band gap of $E_G = 1.42eV$ (at 300K) is given in Fig2.2.

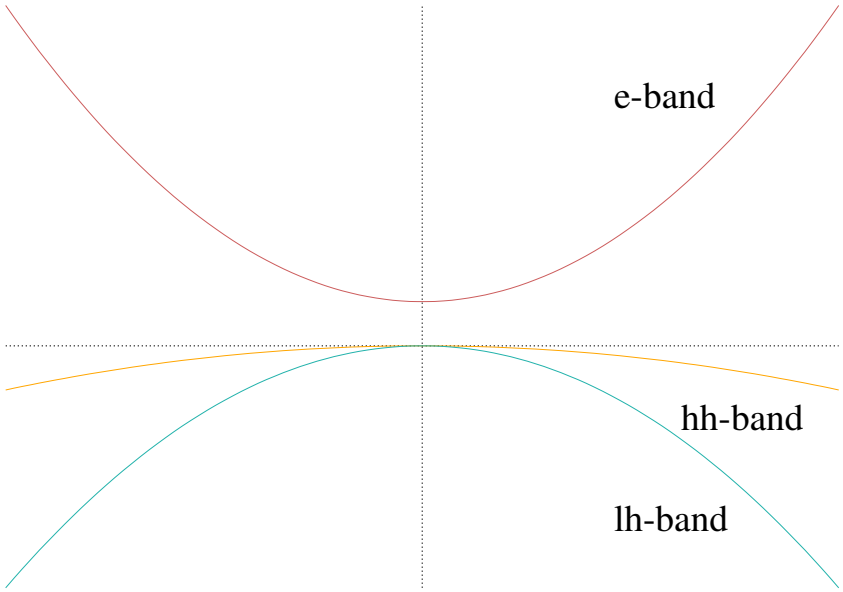

Figure 2.2: Conduction electron and valence heavy hole and light hole bands of GaAs for a band gap of $E_G = 1.42eV$. Horizontal axis is dimensionless wavevector scaled with a_B^2 and vertical axis is energy in units of Hartree energy $E_H = 12meV$.

2.1.3 Dark-bright excitons and radiative couplings

Electrons and holes, being fermions, have their spin, $S = 1/2$. Electrons coming from s-like conduction bands carry angular momentum $L = 0$ and heavy holes coming from p-like bands carry angular momentum $L = 1$. This results in electrons with total angular momenta $J = 1/2$ and holes with total angular momenta $J = 3/2$. To be more specific, heavy holes have $J_z = \pm 3/2$ and light holes have $J_z = \pm 1/2$. The lowest energy combinations give the following combinations for the excitons:

$$\begin{aligned} |\uparrow\uparrow\rangle &= |2\ 2\rangle \\ |\downarrow\downarrow\rangle &= |2\ -2\rangle \\ |\uparrow\downarrow\rangle &= |1\ -1\rangle \\ |\downarrow\uparrow\rangle &= |1\ 1\rangle \end{aligned}$$

These combinations give rise to two fundamentally different varieties, i.e. dark and bright excitons. Bright excitons couple to the light with their odd total angular momenta whereas their dark counterparts are invisible to light with their even angular momenta. Different coupling properties of the dark and bright excitons lead to an important result in the condensed phase: Due to the finite life time of excitons, electron-hole pairs recombine and emit radiation in the form of a photon. The emitted photon can interact with the dark and bright exciton branches via the radiative dipole couplings and as the result of this coupling the amount of bright states in the ground state (GS) diminishes drastically, leaving a purely dark GS[9]. Although there are higher order corrections coming from the Shiva diagrams[25, 26] i.e., dark-bright exchange interactions, in detailed balance the GS is dominated by the dark excitons. This resulted in a huge problem for the experiments based on photoluminescence measurements, since dark states do not couple to the light, which delayed the longly sought experimental evidence of the condensed phase until the pioneering work of Butov *et al.*[19]

2.1.4 Fundamental symmetries in excitonic systems

There are two fundamental symmetries for the excitonic systems to consider: fermion exchange symmetry (FX) and time reversal symmetry (TRS)[11, 12]. Let us begin with FX which is analogous to the particle-hole symmetry (PHS). In the excitonic systems if FX is respect then the below relations must hold:

$$\begin{aligned}
\Delta_{\uparrow\uparrow}(\mathbf{k}) &= C\langle e^{\dagger}_{\mathbf{k}\uparrow} h^{\dagger}_{-\mathbf{k}\uparrow}\rangle = C\langle h^{\dagger}_{-\mathbf{k}\uparrow} e^{\dagger}_{\mathbf{k}\uparrow}\rangle = -\Delta_{\uparrow\uparrow}(-\mathbf{k}) \\
\Delta_{\uparrow\downarrow}(\mathbf{k}) &= C\langle e^{\dagger}_{\mathbf{k}\uparrow} h^{\dagger}_{-\mathbf{k}\downarrow}\rangle = C\langle h^{\dagger}_{-\mathbf{k}\downarrow} e^{\dagger}_{\mathbf{k}\uparrow}\rangle = -\Delta_{\downarrow\uparrow}(-\mathbf{k}) \\
\Delta_{\downarrow\uparrow}(\mathbf{k}) &= C\langle e^{\dagger}_{\mathbf{k}\downarrow} h^{\dagger}_{-\mathbf{k}\uparrow}\rangle = C\langle h^{\dagger}_{-\mathbf{k}\uparrow} e^{\dagger}_{\mathbf{k}\downarrow}\rangle = -\Delta_{\uparrow\downarrow}(-\mathbf{k}) \\
\Delta_{\downarrow\downarrow}(\mathbf{k}) &= C\langle e^{\dagger}_{\mathbf{k}\downarrow} h^{\dagger}_{-\mathbf{k}\downarrow}\rangle = C\langle h^{\dagger}_{-\mathbf{k}\downarrow} e^{\dagger}_{\mathbf{k}\downarrow}\rangle = -\Delta_{\downarrow\downarrow}(-\mathbf{k})
\end{aligned}$$

where $\Delta_{\sigma\sigma'}$ denotes the order parameter (OP) for the exciton condensate, C includes all of terms relating thermodynamic average of fermionic operators to the OP that are absent in the above equation and $\uparrow$ / $\downarrow$ denotes spin quantum numbers. So when we have FX, using the above equation we can write:

$$\bar{\Delta}(\mathbf{k}) = -\bar{\mathbf{\Delta}}^{\mathbf{T}}(-\mathbf{k}), \qquad \bar{\mathbf{\Delta}}(\mathbf{k}) = \begin{pmatrix} \Delta_{\uparrow\uparrow}(\mathbf{k}) & \Delta_{\uparrow\downarrow}(\mathbf{k}) \\ \Delta_{\downarrow\uparrow}(\mathbf{k}) & \Delta_{\downarrow\downarrow}(\mathbf{k}) \end{pmatrix} \tag{2.8}$$

At this point, the interaction will determine whether we will have singlet or triplet states in our system. If we have an even interaction for instance, we have:

$$\bar{\Delta}(\mathbf{k}) = \bar{\mathbf{\Delta}}(-\mathbf{k}) \tag{2.9}$$

In that case, $\Delta_{\uparrow\uparrow}(\mathbf{k}) = \Delta_{\downarrow\downarrow}(\mathbf{k}) = 0$ and $\Delta_{\uparrow\downarrow}(\mathbf{k}) = -\Delta_{\downarrow\uparrow}(\mathbf{k})$ so we have real singlet terms surviving, with all triplet terms vanishing. This is exactly what we have in the case of conventional superconductivity (CSC). If FX were absent in CSC, then one would need to include the triplet terms in addition to the real singlet OP. In the opposite case, an odd interaction yields:

$$\bar{\Delta}(\mathbf{k}) = -\bar{\mathbf{\Delta}}(-\mathbf{k}) \tag{2.10}$$

which gives $\Delta_{\uparrow\downarrow}(\mathbf{k}) = \Delta_{\downarrow\uparrow}(\mathbf{k})$ leaving $d_z \neq 0$, $\Delta_{\uparrow\uparrow}(\mathbf{k})$ and $\Delta_{\downarrow\downarrow}(\mathbf{k})$. Let us now move to the other important symmetry within the context of EC, which is TRS.

Time reversal operator $\hat{\Theta}$ is an antiunitary operator and has three effects on a complex function: it complex conjugates it, it inverts the wavevector $\mathbf{k}$ and it

inverts the spin σ. Because of its antiunitary nature, $\hat{\theta}^2 = -1$ which gives rise to the following: $\hat{\theta}:\uparrow = -\downarrow$ and $\hat{\theta}:\downarrow = \uparrow$. The choice of the minus sign in the former equation here is arbitrary and can also be put in the latter equation instead. Considering these carefully, we have:

$$\hat{\Theta}:\begin{pmatrix}\Delta_{\uparrow\uparrow}(\mathbf{k}) & \Delta_{\uparrow\downarrow}(\mathbf{k})\\ \Delta_{\downarrow\uparrow}(\mathbf{k}) & \Delta_{\downarrow\downarrow}(\mathbf{k})\end{pmatrix} = \begin{pmatrix}\Delta^*_{\downarrow\downarrow}(-\mathbf{k}) & -\Delta^*_{\downarrow\uparrow}(-\mathbf{k})\\ -\Delta^*_{\uparrow\downarrow}(-\mathbf{k}) & \Delta_{\uparrow\uparrow}(-\mathbf{k})\end{pmatrix} \tag{2.11}$$

Again the interaction determines the destiny of the singlet and triplet OPs. In the case of a real even interaction we have, $\Delta_{\uparrow\uparrow}(\mathbf{k}) = \Delta_{\downarrow\downarrow}(\mathbf{k})$ and $\Delta_{\uparrow\downarrow}(\mathbf{k}) = -\Delta_{\downarrow\uparrow}(\mathbf{k})$, a real odd interaction yields $\Delta_{\uparrow\uparrow}(\mathbf{k}) = \Delta_{\downarrow\downarrow}(-\mathbf{k})$ and $\Delta_{\uparrow\downarrow}(\mathbf{k}) = \Delta_{\downarrow\uparrow}(\mathbf{k})$. Finally lets investigate FX and TRS together.

When both FX and TRS manifest and we have a real even interaction we end up with a real singlet: $\Delta_{\uparrow\uparrow}(\mathbf{k}) = \Delta_{\downarrow\downarrow}(\mathbf{k}) = 0$ and $\Delta_{\uparrow\downarrow}(\mathbf{k}) = -\Delta_{\downarrow\uparrow}(\mathbf{k})$. For the case of real odd interaction $\Delta_{\uparrow\uparrow}(\mathbf{k}) = -\Delta_{\downarrow\downarrow}(\mathbf{k})$ and $\Delta_{\uparrow\downarrow}(\mathbf{k}) = \Delta_{\downarrow\uparrow}(\mathbf{k})$

Lets conclude this section by briefly talking about the cases when these symmetries are manifest or broken. The FX is broken in the DQW excitonic systems since there are two species of fermions in excitonic systems. The FX can be manifest in double layer systems with half filled wells, but in that case it is more convenient to talk about PHS instead of FX. The TRS is manifest in the absence of magnetic field but it can also be spontaneously broken.

2.2 Bose-Einstein Condensation of excitons

2.2.1 GaAs DQW geometry

We will use two different geometries; GaAs DQW geometry and $1T\text{-}TiSe_2$, a layered transition metal dichalcogenide. Let us reserve the latter one for later and briefly discuss the former one for now. The GaAs DQW geometry consists of two

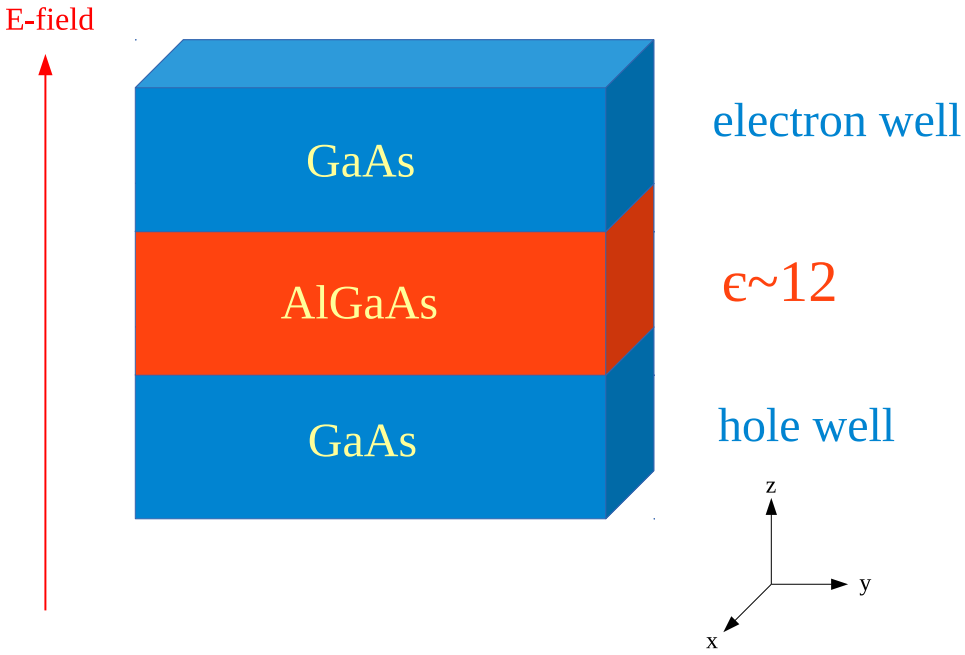

Figure 2.3: Coupled quantum wells of GaAs with the dielectric material $AlGaAs$ for realizing EC state. An electric field $\mathbf{E} \simeq 50kV/cm$ is applied in the growth (z) direction to enhance the lifetime of the excitons.

GaAs quantum wells and a dielectric material, $AlGaAs$ in between, separating the wells. Typical values for the separation is $\sim 100\mathring{A}$. First a laser is shone to create the electron hole pairs. Since electrons and holes tend to recombine, the lifetime of excitons is extremely short, on the order of nano meters. An electric field with magnitude $\simeq 50kV/cm$ is applied in the growth direction (z-direction), to enhance coupling of the electron hole pairs by tuning the valence p and conduction s bands. By this procedure, nearly a thousand fold enhancement in the lifetime is achieved. Then the system is cooled to the temperatures below the EC transition temperature T_c^{EC}.

2.2.2 Second quantization of some related operators

While dealing with many particle quantum systems, it is advantageous to use the second quantization formalism. Lets start with the kinetic energy operator. In real space, the second quantized kinetic energy is given as (for the discussion of first and second quantization and transition between them there are plenty of references, see for instance Ref.[27]):

$$\hat{H}_0 = \sum_{\sigma} \int \mathbf{dr}\ \psi_\sigma(\mathbf{r}) \varepsilon_r \psi^\dagger_\sigma(\mathbf{r}) \tag{2.12}$$

in which $\varepsilon_r = -\hbar^2/2m\nabla^2_{\mathbf{r}}$, $\psi_\sigma(\mathbf{r})$ and $\psi^\dagger_\sigma(\mathbf{r})$ are the real-space annihilation/creation operators at position $\mathbf{r}$ with spin σ. Now lets write the real space annihilation/creation operators in reciprocal space, using the Bloch basis:

$$\psi_\sigma(\mathbf{r}) = \sum_{\mathbf{k}} e_{\mathbf{k},\sigma} e^{i\mathbf{k}\cdot\mathbf{r}} \tag{2.13}$$

$$\psi^\dagger_\sigma(\mathbf{r}) = \sum_{\mathbf{k}} e^\dagger_{\mathbf{k},\sigma} e^{-i\mathbf{k}\cdot\mathbf{r}} \tag{2.14}$$

in the above equations $e_{\mathbf{k},\sigma}/e^\dagger_{\mathbf{k},\sigma}$ are the annihilation/creation operators with momentum $\mathbf{k}$ and spin σ. Plugging those Fourier transformations into Eq.(2.12), we have:

$$\begin{aligned}
\hat{H}_0 &= \sum_{\mathbf{k},\mathbf{k}',\sigma} e^{i\mathbf{k}\cdot\mathbf{r}} \Big(-\frac{\hbar^2}{2m} \nabla^2_{\mathbf{r}} e^{-i\mathbf{k}'\cdot\mathbf{r}} \Big) e_{\mathbf{k},\sigma} e^\dagger_{\mathbf{k}',\sigma} \\
&= \sum_{\mathbf{k},\mathbf{k}',\sigma} \varepsilon_{\mathbf{k}}\ \delta_{\mathbf{k},\mathbf{k}'} e_{\mathbf{k},\sigma} e^\dagger_{\mathbf{k}',\sigma} \\
\hat{H}_0 &= \sum_{\mathbf{k},\sigma} \varepsilon_{\mathbf{k}}\ e_{\mathbf{k},\sigma} e^\dagger_{\mathbf{k},\sigma}
\end{aligned} \tag{2.15}$$

where $\varepsilon_{\mathbf{k}}$ is the energy-momentum dispersion. This is the most general form of the second quantized kinetic energy operator. Now lets move on to the derivation of the most general two-body interaction term in second quantized language with the only condition that $v(\mathbf{r}-\mathbf{r}')$ depends only on $|\mathbf{r}-\mathbf{r}'|$:

$$\hat{H}_1 = \frac{1}{2} \sum_{\sigma,\sigma'} \int \mathbf{dr} \int \mathbf{dr}'\ \psi_\sigma(\mathbf{r}) \psi^\dagger_\sigma(\mathbf{r}) v(\mathbf{r}-\mathbf{r}') \psi_{\sigma'}(\mathbf{r}') \psi^\dagger_{\sigma'}(\mathbf{r}') \tag{2.16}$$

Factor of 1/2 is introduced to avoid double counting. Again expanding the real space operators in the Bloch basis:

$$\hat{H}_1 = \frac{1}{2} \sum_{\sigma,\sigma'} \sum_{\mathbf{k_1},\mathbf{k_2},\mathbf{k_3},\mathbf{k_4}} \int \mathbf{dr} \int \mathbf{dr}'\ e^{i(\mathbf{k_1}-\mathbf{k_2})\cdot\mathbf{r}} v(\mathbf{r}-\mathbf{r}') \times$$

$$e^{i(\mathbf{k_3}-\mathbf{k_4})\cdot\mathbf{r}'} e_{\mathbf{k_1},\sigma} e^{\dagger}_{\mathbf{k_2},\sigma} e_{\mathbf{k_3},\sigma'} e^{\dagger}_{\mathbf{k_4},\sigma'} \tag{2.17}$$

At this point we will use a Jacobian preserving transformation by defining $\mathbf{r}_- = \mathbf{r}-\mathbf{r}'$ and $\mathbf{r}_+ = (\mathbf{r}+\mathbf{r}')/2$. Recasting the above equation using this transformation yields:

$$\hat{H}_1 = \frac{1}{2}\sum_{\sigma,\sigma'}\sum_{\mathbf{k_1},\mathbf{k_2},\mathbf{k_3},\mathbf{k_4}} \int \mathbf{dr}_+ \int \mathbf{dr}_- \; e^{\frac{i}{2}(\mathbf{k_1}-\mathbf{k_2}-\mathbf{k_3}+\mathbf{k_4})\cdot\mathbf{r}_-} v(\mathbf{r}_+) \times e^{i(\mathbf{k_1}-\mathbf{k_2}+\mathbf{k_3}-\mathbf{k_4})\cdot\mathbf{r}_+} e_{\mathbf{k_1},\sigma} e^{\dagger}_{\mathbf{k_2},\sigma} e_{\mathbf{k_3},\sigma'} e^{\dagger}_{\mathbf{k_4},\sigma'} \tag{2.18}$$

Fourier transforming the interaction term and using the spectral definition of the delta function we have:

$$\hat{H}_1 = \frac{1}{2\mathcal{A}}\sum_{\sigma,\sigma'}\sum_{\mathbf{k},\mathbf{k_1},\mathbf{k_2},\mathbf{k_3},\mathbf{k_4}} v(\mathbf{k})\delta_{\mathbf{2k}+\mathbf{k_1}-\mathbf{k_2}-\mathbf{k_3}+\mathbf{k_4}}\delta_{\mathbf{k_1}-\mathbf{k_2}+\mathbf{k_3}-\mathbf{k_4}} \mathbf{e}_{\mathbf{k_1},\sigma}\mathbf{e}^{\dagger}_{\mathbf{k_2},\sigma}\mathbf{e}_{\mathbf{k_3},\sigma'}\mathbf{e}^{\dagger}_{\mathbf{k_4},\sigma'} \tag{2.19}$$

where $\mathcal{A}$ is the area and comes from the Fourier transform of $v(\mathbf{r}_+)$ (since we will be dealing with effectively 2D systems, the derivations are made for that case). Performing the $\mathbf{k_4}$ and $\mathbf{k_2}$ sums by respecting the momentum conservation conditions, $\mathbf{k_4} = -2\mathbf{k}-\mathbf{k_1}+\mathbf{k_2}+\mathbf{k_3}$ and $\mathbf{k_2} = \mathbf{k}+\mathbf{k_1}$ we obtain the final expression for the second quantized two body interaction:

$$\hat{H}_1 = \frac{1}{2\mathcal{A}}\sum_{\sigma,\sigma'}\sum_{\mathbf{k},\mathbf{k}',\mathbf{q}} v(\mathbf{q}) e^{\dagger}_{\mathbf{k}+\mathbf{q},\sigma} e^{\dagger}_{\mathbf{k}'-\mathbf{q},\sigma'} e_{\mathbf{k}',\sigma'} e_{\mathbf{k},\sigma} \tag{2.20}$$

in which, dummy indices are redefined and anticommutation relations of fermionic operators are used. Factors of 2π's coming from the Fourier transformations are omitted during these derivations, since they cancel out with the 2π's coming from Kronecker deltas.

2.2.3 Hartree-Fock mean field approximation

We will use the general two-body interaction in Eq. (2.20) to describe the excitonic systems. One difficulty arises when we want to calculate the eigenspectrum of our system. The problem appears due to the four fermionic operators in $\hat{H}_1$. Using the so called Hartree-Fock mean field approximation, in which we are going to

neglect the fluctuations of order two, we can recast the second quantized two-body interaction term in a form that allows us to solve it self-consistently. To do so, lets first rewrite the most general case of four fermionic operators:

$$e^\dagger_{\mathbf{k}} e_{\mathbf{k}} e^\dagger_{\mathbf{k}'} e_{\mathbf{k}'} = e^\dagger_{\mathbf{k}} e_{\mathbf{k}} \langle e^\dagger_{\mathbf{k}'} e_{\mathbf{k}'} \rangle + \langle e^\dagger_{\mathbf{k}} e_{\mathbf{k}} \rangle e^\dagger_{\mathbf{k}'} e_{\mathbf{k}'} - \langle e^\dagger_{\mathbf{k}} e_{\mathbf{k}} \rangle \langle e^\dagger_{\mathbf{k}'} e_{\mathbf{k}'} \rangle + \sigma_{\mathbf{k}} \sigma_{\mathbf{k}'} \qquad (2.21)$$

where $\sigma_{\mathbf{k}} = e^\dagger_{\mathbf{k}} e_{\mathbf{k}} - \langle e^\dagger_{\mathbf{k}} e_{\mathbf{k}} \rangle$ is the fluctuations of $e^\dagger_{\mathbf{k}} e_{\mathbf{k}}$ around its mean. The last term in the above equation is second order in fluctuations so we neglect that term. The third term does not affect the diagonalization of the Hamiltonian, it only contributes to the total energy. We will see that in the case of exciton condensation (EC), this term is going to be the condensation (free) energy. So we can also drop this term out while calculating the eigenspectrum of our Hamiltonian. The remaining two terms, together with the equations for $\langle e^\dagger_{\mathbf{k}} e_{\mathbf{k}} \rangle$ and $\langle e^\dagger_{\mathbf{k}'} e_{\mathbf{k}'} \rangle$, can be solved self-consistently. The equations for these thermodynamic averages corresponds to the (OP) equations for the ordered systems, which in our case is the equation for the EC OP.

2.2.4 Derivation of the EC Hamiltonian

Now we are in a position to present a microscopic theory for the EC. Our Hamiltonian consists of kinetic energy terms for the electrons and holes and the Coulomb interaction term:

$$\begin{aligned}
\hat{\mathcal{H}} &= \hat{H}^{(e)} + \hat{H}^{(h)} + \hat{H}^{(eh)} \\
\hat{H}^{(e)} &= \sum_{\mathbf{k}\sigma} \xi^{(e)}_{\mathbf{k}} e^\dagger_{\mathbf{k},\sigma} e_{\mathbf{k},\sigma} \\
\hat{H}^{(h)} &= \sum_{\mathbf{k}\sigma} \xi^{(h)}_{\mathbf{k}} h^\dagger_{-\mathbf{k},\sigma} h_{-\mathbf{k},\sigma} \\
\hat{H}^{(eh)} &= \frac{1}{\mathcal{A}} \sum_{\sigma,\sigma'} \sum_{\mathbf{k},\mathbf{k}',\mathbf{q}} v_{eh}(\mathbf{q}) e^\dagger_{\mathbf{k}+\mathbf{q},\sigma} h^\dagger_{\mathbf{k}'-\mathbf{q},\sigma'} e_{\mathbf{k}',\sigma'} h_{\mathbf{k},\sigma}
\end{aligned}$$

with,

$$\begin{aligned}
\xi^{(e)}_{\mathbf{k}} &= \frac{\hbar^2 k^2}{2m^*_e} - \mu_e + \Sigma^{(e)}_{\mathbf{k}} \\
\xi^{(h)}_{\mathbf{k}} &= \frac{\hbar^2 k^2}{2m^*_h} - \mu_h + \Sigma^{(h)}_{\mathbf{k}}
\end{aligned}$$

where $v_{eh}(\mathbf{q}) = -e^2 e^{-|\mathbf{k}-\mathbf{k}'|D}/(2\epsilon|\mathbf{k}-\mathbf{k}'|)$ is the Fourier transform of the Coulomb potential $v(\mathbf{r}-\mathbf{r}') = e^2/(4\pi\epsilon|\mathbf{r}-\mathbf{r}'-D\mathbf{e}_z|)$, with D being the layer separation between the electron and hole wells, μ_e and μ_h are the electron and hole chemical potentials, $\Sigma^{(e)}_{\mathbf{k}}$ and $\Sigma^{(h)}_{\mathbf{k}}$ are the electron and hole self energies which we will derive next together with the Coulomb term using Hartree-Fock mean field theory. For the EC order, the pairings with lowest energies are of those with zero center of mass momentum, i.e. we have $\mathbf{k}' = -\mathbf{k}$. Eliminating the $\mathbf{k}'$ sum and rearranging the indices we have the following for the interaction term:

$$\hat{H}^{(eh)} = \frac{1}{\mathcal{A}} \sum_{\sigma,\sigma'} \sum_{\mathbf{k},\mathbf{k}'} v_{eh}(\mathbf{k}-\mathbf{k}') e^{\dagger}_{\mathbf{k}',\sigma} h^{\dagger}_{-\mathbf{k}',\sigma'} e_{\mathbf{k},\sigma'} h_{\mathbf{k},\sigma} \tag{2.22}$$

The self energy terms arise from the elecron-electron type of interactions with the condition $\mathbf{k}' = \mathbf{k}+\mathbf{q}$ and is given by:

$$\hat{H}^{(ee)} = \frac{1}{2\mathcal{A}} \sum_{\sigma,\sigma'} \sum_{\mathbf{k},\mathbf{k}'} v_{ee}(\mathbf{k}-\mathbf{k}') e^{\dagger}_{\mathbf{k}',\sigma} h^{\dagger}_{\mathbf{k}',\sigma'} e_{\mathbf{k},\sigma'} h_{\mathbf{k},\sigma} \tag{2.23}$$

Here the electron-electron interaction given by $v_{ee}(\mathbf{k}-\mathbf{k}') = -e^2/(2\epsilon|\mathbf{k}-\mathbf{k}'|)$ is Using the mean field approach on the above equations we obtain the final form of our Hamiltonian:

$$\hat{\mathcal{H}} = \sum_{\mathbf{k}\sigma\sigma'} \left[\xi^{(e)}_{\mathbf{k}} e^{\dagger}_{\mathbf{k},\sigma} e_{\mathbf{k},\sigma} + \xi^{(h)}_{\mathbf{k}} h^{\dagger}_{-\mathbf{k},\sigma} h_{-\mathbf{k},\sigma} + \Delta_{\sigma\sigma'}(\mathbf{k}) e_{\mathbf{k},\sigma} h_{\mathbf{k},\sigma} + h.c \right] \tag{2.24}$$

$$\Delta_{\sigma\sigma'}(\mathbf{k}) = \frac{1}{\mathcal{A}} \sum_{\mathbf{k}'} v_{eh}(\mathbf{k}-\mathbf{k}') \langle e^{\dagger}_{\mathbf{k}',\sigma} h^{\dagger}_{-\mathbf{k}',\sigma'} \rangle \tag{2.25}$$

$$\Sigma^{(e)}_{\mathbf{k}} = \frac{1}{2\mathcal{A}} \sum_{\mathbf{k}'} v_{ee}(\mathbf{k}-\mathbf{k}') \langle e^{\dagger}_{\mathbf{k}',\sigma} e_{\mathbf{k}',\sigma} \rangle \tag{2.26}$$

$$\Sigma^{(h)}_{\mathbf{k}} = \frac{1}{2\mathcal{A}} \sum_{\mathbf{k}'} v_{ee}(\mathbf{k}-\mathbf{k}') \langle h^{\dagger}_{\mathbf{k}',\sigma} h_{\mathbf{k}',\sigma} \rangle \tag{2.27}$$

where $\Delta_{\sigma\sigma'}(\mathbf{k})$ are the EC OPs and the constant term $\langle e^{\dagger}_{\mathbf{k}',\sigma} h^{\dagger}_{-\mathbf{k}',\sigma'} \rangle \langle e_{\mathbf{k},\sigma'} h_{\mathbf{k},\sigma} \rangle$ coming from the mean field approximation is omitted. We will concentrate on this term while calculating the EC force.

Chapter 3

Exciton Condensates Under Weak B-field

3.1 Introduction

Excitonic systems present quite a wide spectrum of interesting features thanks to the absence/presence of FX symmetry, unconventional coupling between two species of fermions, **k**-dependent OP and manipulation of the GS by the external fields. For instance, when a magnetic field is turned on, TRS is broken and the Kramers degeneracy in the eigenspectrum is lifted. A more interesting phenomenon in that case is the robustness of the condensed GS against the weak fields: The GS remains unchanged until a critical field strength is reached. When this critical field strength B_c is reached, another significant result is obtained where instabilities arise yielding negative energy states, i.e de-excitation pockets (DX-pockets)[30]. These states are analogous to the negative energy states reported by Sarma in the early 60's[31]. Analytical studies of these instabilities, i.e. Sarma-I and Sarma-II phases and also LOFF phases were reported for the atomic condensates[32, 33, 34, 35, 36]. LOFF phases are not included in this thesis, which are instabilities arising from non-zero center of mass momentum pairings, which

can be triggered by a strong magnetic field in superconductor systems for instance and requires real space diagonalization, which was not achieved for the EC systems yet to our knowledge.

3.2 Robust Ground State and the DX-pockets

3.2.1 Microscopic theory

Lets recast Eq.(2.24) in the matrix form using the $(e^{\dagger}_{\mathbf{k}\uparrow}e^{\dagger}_{\mathbf{k}\downarrow}h_{-\mathbf{k}\uparrow}h_{-\mathbf{k}\downarrow})$ basis:

$$\hat{\mathcal{H}} = \sum_{\mathbf{k}} \begin{pmatrix} \xi^{(e)}_{\mathbf{k}} & 0 & \Delta^{*}_{\uparrow\uparrow}(\mathbf{k}) & \Delta^{*}_{\downarrow\uparrow}(\mathbf{k}) \\ 0 & \xi^{(e)}_{\mathbf{k}} & \Delta^{*}_{\uparrow\downarrow}(\mathbf{k}) & \Delta^{*}_{\downarrow\downarrow}(\mathbf{k}) \\ \Delta_{\uparrow\uparrow}(\mathbf{k}) & \Delta_{\uparrow\downarrow}(\mathbf{k}) & \xi^{(h)}_{\mathbf{k}} & 0 \\ \Delta_{\downarrow\uparrow}(\mathbf{k}) & \Delta_{\downarrow\downarrow}(\mathbf{k}) & 0 & \xi^{(h)}_{\mathbf{k}} \end{pmatrix} \tag{3.1}$$

By defining $\varepsilon^{(+)}_{\mathbf{k}} = (\xi^{(e)}_{\mathbf{k}} + \xi^{(h)}_{\mathbf{k}})/2$ and $\varepsilon^{(-)}_{\mathbf{k}} = (\xi^{(e)}_{\mathbf{k}} - \xi^{(h)}_{\mathbf{k}})/2$ we can rewrite the above equation in the following form:

$$\hat{\mathcal{H}} = \sum_{\mathbf{k}} \left\{ \varepsilon^{(-)}_{\mathbf{k}}\sigma_0 \otimes \sigma_0 + \begin{pmatrix} \varepsilon^{(+)}_{\mathbf{k}}\sigma_0 & \bar{\Delta}^{\dagger}(\mathbf{k}) \\ \bar{\Delta}(\mathbf{k}) & -\varepsilon^{(-)}_{\mathbf{k}}\sigma_0 \end{pmatrix} \right\} \tag{3.2}$$

in which σ_0 is the 2×2 unit matrix, $\bar{\Delta}(\mathbf{k})$ is the OP matrix[28], which was also introduced in the previous chapter. The energy spectrum of the above Hamiltonian is two-fold degenerate and given by:

$$\lambda^{(\pm)}_{\mathbf{k}} = \varepsilon^{(-)}_{\mathbf{k}} \pm \lambda_{\mathbf{k}} = \varepsilon^{(-)}_{\mathbf{k}} \pm \sqrt{[\varepsilon^{(+)}_{\mathbf{k}}]^2 + tr[\bar{\Delta}(\mathbf{k})\bar{\Delta}^{\dagger}(\mathbf{k})]/2} \tag{3.3}$$

To find the eigenfunctions, we need to diagonalize this Hamiltonian. For that, we will resort to an unitary transformation:

$$\hat{U}\hat{\mathcal{H}}\hat{U}^{\dagger} = \hat{\mathcal{H}}_d \tag{3.4}$$

where $\hat{\mathcal{H}}_d$ is the diagonalized Hamiltonian, and $\hat{U}$ is the unitary transformation we are using and are given by:

$$\hat{\mathcal{H}}_d = \begin{pmatrix} \lambda_{\mathbf{k}}\sigma_0 & 0 \\ 0 & -\lambda_{\mathbf{k}}\sigma_0 \end{pmatrix}, \qquad \hat{U} = \begin{pmatrix} \alpha_{\mathbf{k}} & 0 & \beta_{\mathbf{k}} & \gamma_{\mathbf{k}} \\ 0 & \alpha_{\mathbf{k}} & -\gamma_{\mathbf{k}} & \beta_{\mathbf{k}} \\ -\beta_{\mathbf{k}} & \gamma_{\mathbf{k}} & \alpha_{\mathbf{k}} & 0 \\ -\gamma_{\mathbf{k}} & -\beta_{\mathbf{k}} & 0 & \alpha_{\mathbf{k}} \end{pmatrix} \tag{3.5}$$

Multiplying both sides of Eq.(3.4) by $\hat{U}$ from the right, we have a set of equations for $\alpha_{\mathbf{k}}$, $\beta_{\mathbf{k}}$ and $\gamma_{\mathbf{k}}$. Combining these with the equations coming from the unitarity condition $\hat{U}\hat{U}^{\dagger} = \sigma_0 \otimes \sigma_0$ we have:

$$\begin{aligned} \alpha_{\mathbf{k}} &= C_{\mathbf{k}}[\lambda_{\mathbf{k}} + \varepsilon_{\mathbf{k}}^{(+)}] \\ \beta_{\mathbf{k}} &= C_{\mathbf{k}}\Delta_{\uparrow\uparrow}(\mathbf{k}) \\ \gamma_{\mathbf{k}} &= C_{\mathbf{k}}\Delta_{\uparrow\downarrow}(\mathbf{k}) \\ C_{\mathbf{k}} &= \frac{1}{\sqrt{2\lambda_{\mathbf{k}}[\lambda_{\mathbf{k}} + \varepsilon_{\mathbf{k}}^{(+)}]}} \end{aligned}$$

Since we determined the elements of $\hat{U}$ we can now also find the new basis in which our Hamiltonian is diagonal:

$$\begin{pmatrix} g_{1\mathbf{k}} \\ g_{2\mathbf{k}} \\ g_{3\mathbf{k}}^{\dagger} \\ g_{4\mathbf{k}}^{\dagger} \end{pmatrix} = \begin{pmatrix} \alpha_{\mathbf{k}} & 0 & \beta_{\mathbf{k}} & \gamma_{\mathbf{k}} \\ 0 & \alpha_{\mathbf{k}} & -\gamma_{\mathbf{k}} & \beta_{\mathbf{k}} \\ -\beta_{\mathbf{k}} & \gamma_{\mathbf{k}} & \alpha_{\mathbf{k}} & 0 \\ -\gamma_{\mathbf{k}} & -\beta_{\mathbf{k}} & 0 & \alpha_{\mathbf{k}} \end{pmatrix} \begin{pmatrix} e_{\mathbf{k}\uparrow} \\ e_{\mathbf{k}\downarrow} \\ h_{-\mathbf{k}\uparrow}^{\dagger} \\ h_{-\mathbf{k}\downarrow}^{\dagger} \end{pmatrix} \tag{3.6}$$

multiplying by $\hat{U}^{\dagger}$ from the left we can also express our old basis in terms of the new one:

$$\begin{pmatrix} e_{\mathbf{k}\uparrow} \\ e_{\mathbf{k}\downarrow} \\ h_{-\mathbf{k}\uparrow}^{\dagger} \\ h_{-\mathbf{k}\downarrow}^{\dagger} \end{pmatrix} = \begin{pmatrix} \alpha_{\mathbf{k}} & 0 & -\beta_{\mathbf{k}} & -\gamma_{\mathbf{k}} \\ 0 & \alpha_{\mathbf{k}} & \gamma_{\mathbf{k}} & -\beta_{\mathbf{k}} \\ \beta_{\mathbf{k}} & -\gamma_{\mathbf{k}} & \alpha_{\mathbf{k}} & 0 \\ \gamma_{\mathbf{k}} & \beta_{\mathbf{k}} & 0 & \alpha_{\mathbf{k}} \end{pmatrix} \begin{pmatrix} g_{1\mathbf{k}} \\ g_{2\mathbf{k}} \\ g_{3\mathbf{k}}^{\dagger} \\ g_{4\mathbf{k}}^{\dagger} \end{pmatrix} \tag{3.7}$$

or in open form:

$$\begin{aligned} e_{\mathbf{k}\uparrow} &= \alpha_{\mathbf{k}} g_{1\mathbf{k}} - \beta_{\mathbf{k}} g_{3\mathbf{k}}^{\dagger} - \gamma_{\mathbf{k}} g_{4\mathbf{k}}^{\dagger} \\ e_{\mathbf{k}\downarrow} &= \alpha_{\mathbf{k}} g_{2\mathbf{k}} + \gamma_{\mathbf{k}} g_{3\mathbf{k}}^{\dagger} - \beta_{\mathbf{k}} g_{4\mathbf{k}}^{\dagger} \\ h_{-\mathbf{k}\uparrow}^{\dagger} &= \beta_{\mathbf{k}} g_{1\mathbf{k}} - \gamma_{\mathbf{k}} g_{2\mathbf{k}} - \alpha_{\mathbf{k}} g_{3\mathbf{k}}^{\dagger} \\ h_{-\mathbf{k}\downarrow}^{\dagger} &= \gamma_{\mathbf{k}} g_{1\mathbf{k}} + \beta_{\mathbf{k}} g_{2\mathbf{k}} + \alpha_{\mathbf{k}} g_{4\mathbf{k}}^{\dagger} \end{aligned}$$

and similarly for the quasiparticle operators we have:

$$\begin{aligned} g_{1\mathbf{k}} &= \alpha_{\mathbf{k}} e_{\mathbf{k}\uparrow} + \beta_{\mathbf{k}} h_{-\mathbf{k}\uparrow}^{\dagger} + \gamma_{\mathbf{k}} h_{-\mathbf{k}\downarrow}^{\dagger} \\ g_{2\mathbf{k}} &= \alpha_{\mathbf{k}} e_{\mathbf{k}\downarrow} - \gamma_{\mathbf{k}} h_{-\mathbf{k}\uparrow}^{\dagger} + \beta_{\mathbf{k}} h_{-\mathbf{k}\downarrow}^{\dagger} \\ g_{3\mathbf{k}} &= \alpha_{\mathbf{k}} h_{\mathbf{k}\uparrow} - \beta_{\mathbf{k}} e_{-\mathbf{k}\uparrow}^{\dagger} + \gamma_{\mathbf{k}} e_{-\mathbf{k}\downarrow}^{\dagger} \\ g_{4\mathbf{k}} &= \alpha_{\mathbf{k}} h_{\mathbf{k}\downarrow} - \gamma_{\mathbf{k}} e_{-\mathbf{k}\uparrow}^{\dagger} - \beta_{\mathbf{k}} e_{-\mathbf{k}\downarrow}^{\dagger} \end{aligned}$$

By using the TRS transformation properties of the OPs, we can relate the quasiparticle annihilation operators: OPs in our case are real and since the Coulomb potential is even we have: $\hat{\Theta} : \Delta_{\sigma\sigma}(\mathbf{k}) = \Delta_{\bar{\sigma}\bar{\sigma}}(\mathbf{k})$ and $\hat{\Theta} : \Delta_{\sigma\bar{\sigma}}(\mathbf{k}) = -\Delta_{\bar{\sigma}\sigma}(\mathbf{k})$. Using these in the above equations we obtain the following transformations:

$$\begin{aligned}
\hat{\Theta} : g_{1\mathbf{k}} &= g_{2(-\mathbf{k})} \\
\hat{\Theta} : g_{3\mathbf{k}} &= g_{4(-\mathbf{k})} \\
\hat{\Theta} : g_{2\mathbf{k}} &= -g_{1(-\mathbf{k})} \\
\hat{\Theta} : g_{4\mathbf{k}} &= -g_{3(-\mathbf{k})}
\end{aligned}$$

We can express the GS similar to the product state defined in the BCS theory[29] via the vacuum modes:

$$|\Psi_0\rangle = \prod_{\mathbf{k}} |\Psi_{\mathbf{k}}\rangle, \qquad |\Psi_{\mathbf{k}}\rangle = T_{\mathbf{k}}^{(1)} T_{\mathbf{k}}^{(2)} |\mathbf{0}\rangle \tag{3.8}$$

with

$$\begin{aligned}
T_{\mathbf{k}}^{(1)} &= \alpha_{\mathbf{k}} - \beta_{\mathbf{k}} e_{\mathbf{k}\uparrow}^{\dagger} h_{-\mathbf{k}\uparrow}^{\dagger} - \gamma_{\mathbf{k}} e_{\mathbf{k}\uparrow}^{\dagger} h_{-\mathbf{k}\downarrow}^{\dagger} \\
T_{\mathbf{k}}^{(2)} &= \alpha_{\mathbf{k}} - \beta_{\mathbf{k}} e_{\mathbf{k}\downarrow}^{\dagger} h_{-\mathbf{k}\downarrow}^{\dagger} + \gamma_{\mathbf{k}} e_{\mathbf{k}\downarrow}^{\dagger} h_{-\mathbf{k}\uparrow}^{\dagger}
\end{aligned}$$

The ground state has two significant features. Firstly, it is a singlet, i.e. $|\Psi_{\mathbf{k}}\rangle = |\Psi_{-\mathbf{k}}\rangle$ and secondly, it transforms to itself under time reversal.

Before advancing to the derivation of the self consistent set of equations, let us write the diagonalized Hamiltonian via the ground state energy E_G:

$$\hat{\mathcal{H}}_d = E_G + \sum_{\mathbf{k}} [\lambda_{\mathbf{k}}^{(+)} (g_{1\mathbf{k}}^{\dagger} g_{1\mathbf{k}} + g_{2\mathbf{k}}^{\dagger} g_{2\mathbf{k}}) - \lambda_{\mathbf{k}}^{(-)} (g_{3\mathbf{k}}^{\dagger} g_{3\mathbf{k}} + g_{4\mathbf{k}}^{\dagger} g_{4\mathbf{k}})] \tag{3.9}$$

where the ground state energy is given by:

$$E_G = 2 \sum_{\mathbf{k}} \lambda_{\mathbf{k}}^{(-)} \tag{3.10}$$

From this moment, we will take dark and bright EC OPs to be equal by ignoring the radiative coupling which yields: $|\Delta_{\uparrow\uparrow}(\mathbf{k})| = |\Delta_{\downarrow\downarrow}(\mathbf{k})| = |\Delta_{\uparrow\downarrow}(\mathbf{k})| = |\Delta_{\downarrow\uparrow}(\mathbf{k})|$ and denote this single OP simply by $\Delta(\mathbf{k})$. Since we know the transformation between the old and the new basis we can easily cast the OP equation using Eq.(2.25):

$$\Delta(\mathbf{k}) = \frac{1}{2} \int \frac{\mathbf{dk}'}{(2\pi)^2} v(\mathbf{k} - \mathbf{k}') \frac{\Delta(\mathbf{k}')}{2\lambda_{\mathbf{k}'}} [f_1(\mathbf{k}') - f_2(\mathbf{k}')] \tag{3.11}$$

where, $f_1(\mathbf{k})$ and $f_2(\mathbf{k})$ are the Fermi-Dirac functions for energies $\lambda_{\mathbf{k}}^{(+)}$ and $\lambda_{\mathbf{k}}^{(-)}$ respectively. To complete the self consistent set, we need number conservation equations and self energies. Number conservation for the electrons and holes are given by:

$$N^{(e)} = \sum_{\mathbf{k}\sigma} \langle e_{\mathbf{k}\sigma}^{\dagger} e_{\mathbf{k}\sigma} \rangle \tag{3.12}$$

$$N^{(h)} = \sum_{\mathbf{k}\sigma} \langle h_{\mathbf{k}\sigma}^{\dagger} h_{\mathbf{k}\sigma} \rangle \tag{3.13}$$

where $N^{(e)}$ and $N^{(h)}$ are number of electrons and holes respectively. Calculating those thermodynamic averages we have:

$$n^{(e)} = \int \frac{\mathbf{dk}}{(2\pi)^2} \Big[(1 + \frac{\varepsilon_{\mathbf{k}}^{(+)}}{\lambda(\mathbf{k})}) f_1(\mathbf{k}) + (1 - \frac{\varepsilon_{\mathbf{k}}^{(+)}}{\lambda(\mathbf{k})}) f_2(\mathbf{k}) \Big] \tag{3.14}$$

$$n^{(h)} = \int \frac{\mathbf{dk}}{(2\pi)^2} \Big[(1 - \frac{\varepsilon_{\mathbf{k}}^{(+)}}{\lambda(\mathbf{k})}) \Big(1 - f_1(\mathbf{k}) \Big) + (1 + \frac{\varepsilon_{\mathbf{k}}^{(+)}}{\lambda(\mathbf{k})}) \Big(1 - f_2(\mathbf{k}) \Big) \Big] \tag{3.15}$$

in which $n^{(e)} = N^{(e)}/\mathcal{A}$ and $n^{(h)} = N^{(h)}/\mathcal{A}$ are the electron and hole densities. We also need the self energies for the self consistent solution:

$$\Sigma_{\mathbf{k}}^{(e)} = \frac{1}{2} \int \frac{\mathbf{dk'}}{(2\pi)^2} v_{ee}(\mathbf{k} - \mathbf{k'}) \Big[(1 + \frac{\varepsilon_{\mathbf{k}}^{(+)}}{\lambda(\mathbf{k})}) f_1(\mathbf{k}) + (1 - \frac{\varepsilon_{\mathbf{k}}^{(+)}}{\lambda(\mathbf{k})}) f_2(\mathbf{k}) \Big] \tag{3.16}$$

$$\Sigma_{\mathbf{k}}^{(h)} = \frac{1}{2} \int \frac{\mathbf{dk'}}{(2\pi)^2} v_{ee}(\mathbf{k} - \mathbf{k'}) \Big[(1 - \frac{\varepsilon_{\mathbf{k}}^{(+)}}{\lambda(\mathbf{k})}) \Big(1 - f_1(\mathbf{k}) \Big) + (1 + \frac{\varepsilon_{\mathbf{k}}^{(+)}}{\lambda(\mathbf{k})}) \Big(1 - f_2(\mathbf{k}) \Big) \Big] \tag{3.17}$$

Above equations together with the OP equation form a self consistent set for $\Delta(\mathbf{k})$, $\Sigma_{\mathbf{k}}^{(e)}$, $\Sigma_{\mathbf{k}}^{(h)}$, μ_e and μ_h. Alternatively, we can use the exciton density $n^{(+)} = (n^{(e)} + n^{(h)})/2$ and electron-hole density mismatch $n^{(-)} = (n^{(e)} - n^{(h)})/2$ to solve for $\Delta(\mathbf{k})$, $\Sigma_{\mathbf{k}}^{(e)}$, $\Sigma_{\mathbf{k}}^{(h)}$, $\mu_+ = (\mu_e + \mu_h)/2$ and $\mu_- = (\mu_e - \mu_h)/2$ self consistently:

$$n^{(+)} = \int \frac{\mathbf{dk}}{(2\pi)^2} \Big[1 + \frac{\varepsilon_{\mathbf{k}}^{(+)}}{\lambda(\mathbf{k})} [(f_1(\mathbf{k}) - f_2(\mathbf{k}))] \Big] \tag{3.18}$$

$$n^{(-)} = \int \frac{\mathbf{dk}}{(2\pi)^2} \Big[f_1(\mathbf{k}) + f_2(\mathbf{k}) - 1 \Big] \tag{3.19}$$

Following the onset of the condensate we turn on a weak magnetic field $\mathbf{B}(\mathbf{r}) = B_{\perp}\hat{e}_{\phi} + B_z\hat{e}_z$ where the radial and perpendicular components of the magnetic field

$B_\perp$ and $+B_z$ are independent of θ ans ϕ and a slowly varying function of r. We are not considering the effects of the magnetic vector potential which is valid since the magnitude of the magnetic fields we are using are not exceeding and the critical value for the Landau degeneracy, i.e. $|\mathbf{B}(\mathbf{r}) \ll B_0 = \phi_0 n_x$ in which $\phi_0 = h/e$ is the flux quantum. We are also neglecting the the influence of light holes on the heavy hole states[37, 38]. The Zeeman coupling for the electron-heavy hole coupled system is given by:

$$V_z = -(\gamma_e \bar{\sigma}^{(e)} \cdot \mathbf{B}(\mathbf{r}) + \gamma_h \sigma_z^{(h)} B_z) \tag{3.20}$$

with $\bar{\sigma} = \sigma_x \hat{e}_x + \sigma_y \hat{e}_y + \sigma_z \hat{e}_z$ denoting the Pauli matrices, $\gamma_p = g^* \mu_B^*$, $p = (e, h)$ $g^* = \sqrt{g_\perp^2 + g_z^2}$ is the effective g-factor and $\mu_B^* = e\hbar/2m^*$ with m^* being electron and hole effective masses for γ_e and γ_h respectively. We will treat the Zeeman coupling within the first order perturbation theory, and introduce it to the diagonalized EC Hamiltonian in the following manner:

$$\mathcal{H}_B = \mathcal{H}_d + \mathcal{Z}, \qquad \mathcal{Z} = \begin{pmatrix} Z^{(1)} & 0 \\ 0 & Z^{(2)} \end{pmatrix} \tag{3.21}$$

in which $Z^{(i)} = \mathbf{h}^i \cdot \bar{\sigma}$, $\mathbf{h}^i = h_x^{(i)} \hat{e}_x + h_y^{(i)} \hat{e}_y + h_z^{(i)} \hat{e}_z$, $i = (1, 2)$ with $h^{(i)}$'s given by:

$$\begin{aligned} h_x^{(1)} &= \alpha_{\mathbf{k}}^2 \gamma_e B_\perp^{(e)} cos\phi \\ h_y^{(1)} &= \alpha_{\mathbf{k}}^2 \gamma_e B_\perp^{(e)} sin\phi \\ h_z^{(1)} &= \alpha_{\mathbf{k}}^2 \gamma_e B_z^{(e)} - (\beta_{\mathbf{k}}^2 + \gamma_{\mathbf{k}}^2) \gamma_h B_z^{(h)} \end{aligned} \tag{3.22}$$

given in $(g_{1\mathbf{k}}, g_{2\mathbf{k}})$ basis and

$$\begin{aligned} h_x^{(2)} &= (\beta_{\mathbf{k}}^2 + \gamma_{\mathbf{k}}^2) \gamma_e B_\perp^{(e)} cos\phi \\ h_y^{(2)} &= (\beta_{\mathbf{k}}^2 + \gamma_{\mathbf{k}}^2) \gamma_e B_\perp^{(e)} sin\phi \\ h_z^{(2)} &= (\beta_{\mathbf{k}}^2 + \gamma_{\mathbf{k}}^2) \gamma_e B_z^{(e)} - \alpha_{\mathbf{k}}^2 \gamma_h B_z^{(h)} \end{aligned} \tag{3.23}$$

given in $(g_{3\mathbf{k}}^\dagger, g_{4\mathbf{k}}^\dagger)$ basis. The Zeeman field breaks the degeneracy and splits the energy spectrum into four given by: $E_{1\mathbf{k}}^{(\pm)} = \lambda_{\mathbf{k}}^{(+)} \pm z_{\mathbf{k}}^{(1)}$ and $E_{2\mathbf{k}}^{(\pm)} = \lambda_{\mathbf{k}}^{(-)} \pm z_{\mathbf{k}}^{(2)}$ with $z_{\mathbf{k}}^{(1)} = |\mathbf{h}^{(1)}|$ and $z_{\mathbf{k}}^{(2)} = |\mathbf{h}^{(2)}|$. The new basis in which $\mathcal{H}_B$ is diagonal is related to the EC basis via another unitary transformation:

$$\begin{pmatrix} G_{1\mathbf{k}} \\ G_{2\mathbf{k}} \\ G_{3\mathbf{k}} \\ G_{4\mathbf{k}} \end{pmatrix} = \begin{pmatrix} cos\frac{\theta_1}{2} & e^{-i\phi} sin\frac{\theta_1}{2} & 0 & 0 \\ -e^{i\phi} sin\frac{\theta_1}{2} & cos\frac{\theta_1}{2} & 0 & 0 \\ 0 & 0 & cos\frac{\theta_2}{2} & e^{-i\phi} sin\frac{\theta_2}{2} \\ 0 & 0 & -e^{i\phi} sin\frac{\theta_2}{2} & cos\frac{\theta_2}{2} \end{pmatrix} \begin{pmatrix} g_{1\mathbf{k}} \\ g_{2\mathbf{k}} \\ g_{3\mathbf{k}} \\ g_{4\mathbf{k}} \end{pmatrix} \tag{3.24}$$

with $\theta_1 = \sqrt{(h_x^{(1)})^2 + (h_y^{(1)})^2}/h_z^{(1)}$ and $\theta_2 = \sqrt{(h_x^{(2)})^2 + (h_y^{(2)})^2}/h_z^{(2)}$. Now lets recast $\mathcal{H}_B$ in the diagonalized basis:

$$\mathcal{H}_B = E_G + \sum_{\mathbf{k}} [E_{1\mathbf{k}}^{(+)} G_{1\mathbf{k}}^\dagger G_{1\mathbf{k}} + E_{1\mathbf{k}}^{(-)} G_{2\mathbf{k}}^\dagger G_{2\mathbf{k}} - E_{2\mathbf{k}}^{(+)} G_{3\mathbf{k}}^\dagger G_{3\mathbf{k}} - E_{2\mathbf{k}}^{(-)} G_{4\mathbf{k}}^\dagger G_{4\mathbf{k}}] \quad (3.25)$$

in which $E_G = 2\sum_{\mathbf{k}} \lambda_{\mathbf{k}}^{(-)}$ is the same ground state that we found for the $B = 0$ case. The ground state is robust against magnetic field unless $E_{2\mathbf{k}}^{(+)}$ becomes positive or $E_{1\mathbf{k}}^{(-)}$ becomes negative at some $\mathbf{k}$ values for some critical field $\mathbf{B}_c$. When it is the case, E_G is not the ground state anymore and negative excitations, which we call DX-pockets arise. DX-pockets also arise by introducing a nonzero electron-hole density mismatch. All these cases are investigated in the next section. We can again express the new ground state via a product state:

$$|\Psi_B\rangle = \prod_{\{\mathbf{k_1}\}} G_{2\mathbf{k_1}}^\dagger \prod_{\{\mathbf{k_2}\}} G_{3\mathbf{k_2}}^\dagger |\Psi_0\rangle \quad (3.26)$$

in the above equation, $\{\mathbf{k_1}\}$ and $\{\mathbf{k_2}\}$ are the DX-pockets created where $E_{1\mathbf{k}}^{(-)} < 0$ and $E_{2\mathbf{k}}^{(+)} > 0$ respectively. For these $\mathbf{k}$ values it is energetically more favorable to break a pair by the operators $G_{2\mathbf{k}}^\dagger$ and $G_{3\mathbf{k}}^\dagger$ yielding a new ground state with a negative energy. The DX-pockets corresponding to the $E_{1\mathbf{k}}^{(-)}$ branch have $0 < k < Q_1$ and therefore have disk topology whereas the remaining DX-pockets belonging to $E_{2\mathbf{k}}^{(+)}$ branch have $Q_2 < k < Q_3$ and have ring topology as a result, with Q_i's designating the positions of the zero energy crossings. These two topologically different instabilities are analogous to the Sarma-I and Sarma-II phases appearing in the BSC systems[31].

3.2.2 Numerical results

We solved the self consistent set of Eqs.[3.11, 3.14, 3.15, 3.16, 3.17] numerically for a parameter space consisting of the dimensionless parameters $n^{(+)}a_B^2$, $n^{(-)}a_B^2$ and g^*B/B_0. The results are illustrated in Fig. (3.1 - 3.5).

In the absence of electron-hole density mismatch and magnetic field, the ground state is robust and we don't have DX-pockets as shown in Fig. (3.1). As we turn

on the magnetic field, DX-pockets appear for certain k values, which were denoted by $\{\mathbf{k_1}\}$ and $\{\mathbf{k_2}\}$ in the previous section and are shown in Fig. 3.2a/Fig. 3.3a and Fig. 3.2b/Fig. 3.3b, with disk and ring topologies respectively.

The other way to obtain negative energy DX-pockets is to introduce electron-hole density mismatch. When $n^{(-)}a_B^2 \neq 0$, DX-pockets arise for the certain set of $\mathbf{k}$ values, which corresponds to the pairs broken by the operators $G^\dagger_{2\mathbf{k_1}}$ and $G^\dagger_{3\mathbf{k_2}}$. Those cases are shown in Fig. 3.4 and Fig. 3.5.

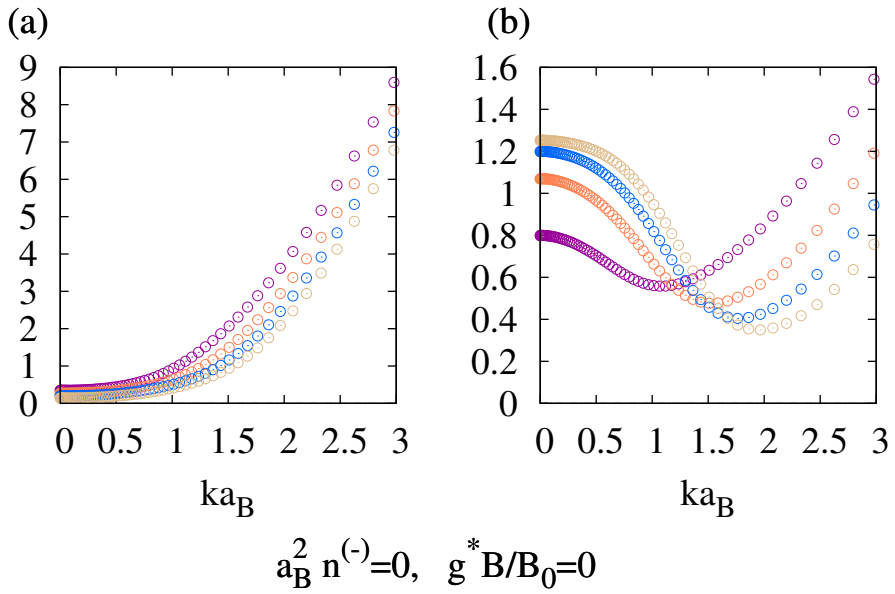

Figure 3.1: $E^{(-)}_{1\mathbf{k}}/E_H$ (a) and $E^{(+)}_{2\mathbf{k}}/E_H$ (b) versus ka_B is plotted for $n^{(+)}a_B^2 = 0.1, 0.3, 0.5, 0.7$ (from bottom to top) at constant $n^{(-)} = 0$ and $g^*B/B_0 = 0$.

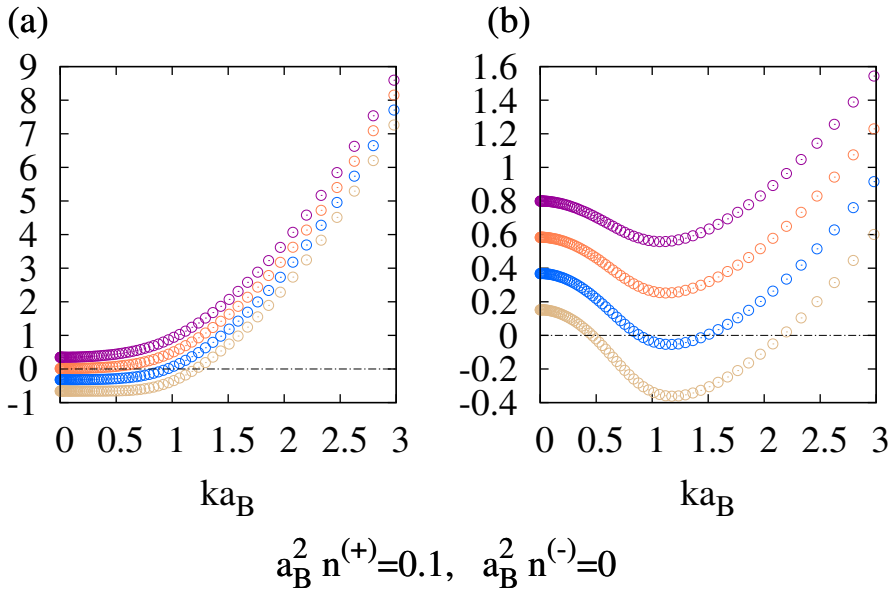

Figure 3.2: $E^{(-)}_{1\mathbf{k}}/E_H$ (a) and $E^{(+)}_{2\mathbf{k}}/E_H$ (b) versus ka_B is plotted for $g^*B/B_0 = 0, 2, 4, 6$ (from top to bottom) at constant $n^{(+)} = 0.1$ and $n^{(-)} = 0$.

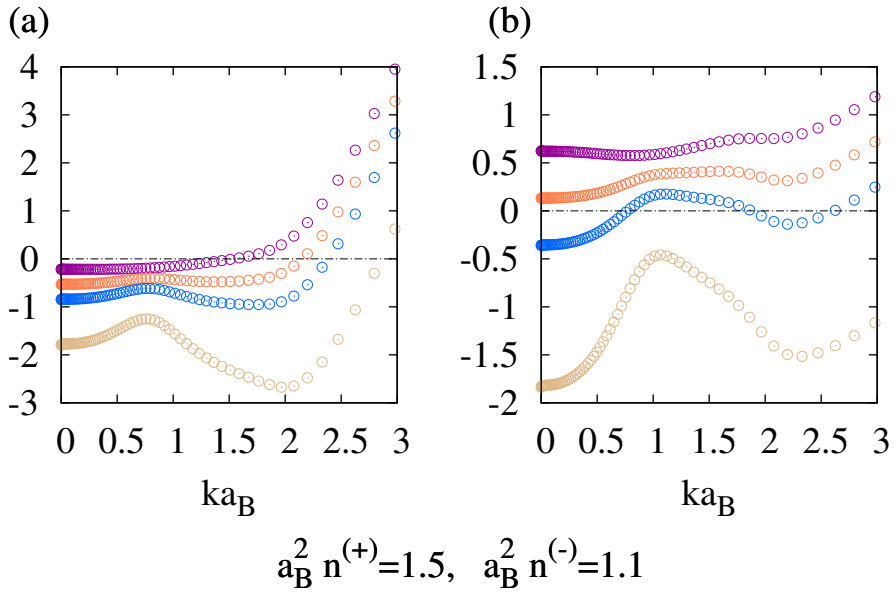

Figure 3.3: $E^{(-)}_{1\mathbf{k}}/E_H$ (a) and $E^{(+)}_{2\mathbf{k}}/E_H$ (b) versus ka_B is plotted for $g^*B/B_0 = 0, 0.2, 0.4, 1$ (from top to bottom) at constant $n^{(+)} = 1.5$ and $n^{(-)} = 1.1$.

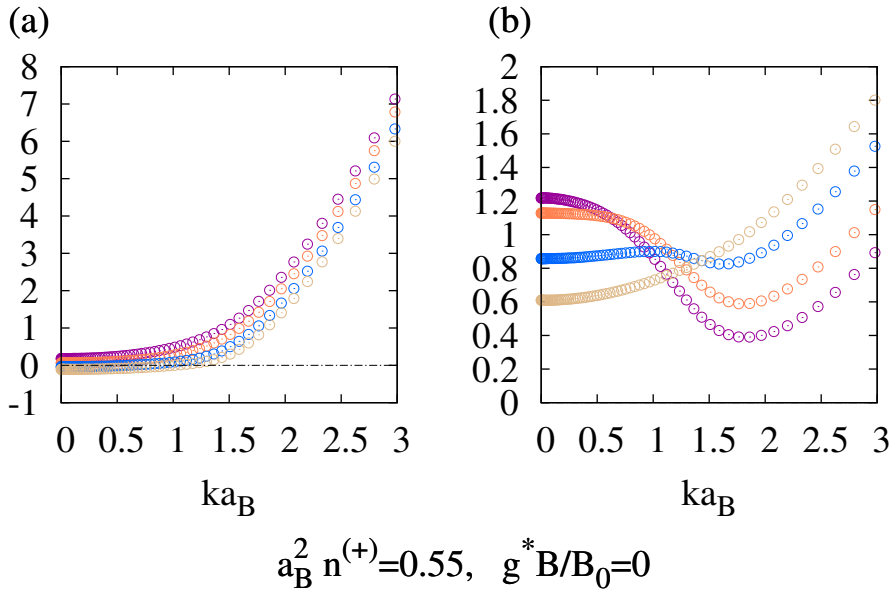

Figure 3.4: $E^{(-)}_{1\mathbf{k}}/E_H$ (a) and $E^{(+)}_{2\mathbf{k}}/E_H$ (b) versus ka_B is plotted for $n^{(-)} = 0, 0.1, 0.3, 0.5$ (from top to bottom) at constant $n^{(+)} = 0.55$ and $g^*B/B_0 = 0$.

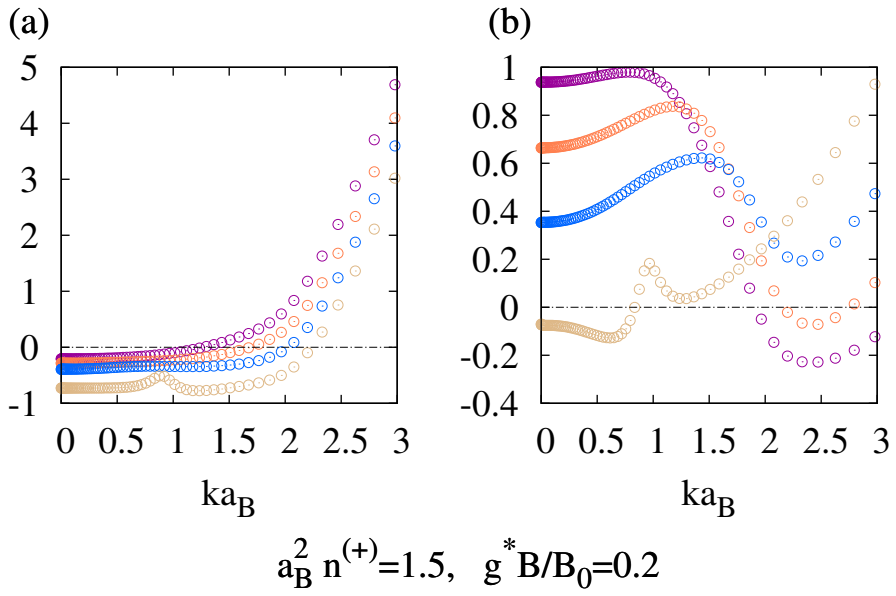

Figure 3.5: $E^{(-)}_{1\mathbf{k}}/E_H$ (a) and $E^{(+)}_{2\mathbf{k}}/E_H$ (b) versus ka_B is plotted for $n^{(-)} = 0, 0.4, 0.8, 1.4$ (from top to bottom) at constant $n^{(+)} = 1.5$ and $g^*B/B_0 = 0.2$.

Chapter 4

The EC force

4.1 Introduction

The main focus of this thesis which is a recently discovered feature of the EC systems arises due to the D- dependence of the condensation free energy. This feature yields a new type of force i.e. EC force[9, 18] which is reminiscent of the attractive Casimir force (CF) arising between infinitely large metallic plates of identical size[39]. An analogous effect is the Critical Casimir force (CCF), which has been predicted[40] and measured experimentally[41, 42, 43] in binary liquid mixtures. CCF in BEC systems was also speculated[44, 45], but has not yet been observed. However, Casimir-Polder like force between a BEC and a semiconductor plane was measured[46, 47].

As we discussed earlier, there exists two different type of excitons, i.e. dark and bright excitons and due to the radiative corrections, bright excitons in the GS is drastically suppressed, leaving a dark GS, which makes photoluminescence experiments inconclusive[10, 48, 49], until the recent observation of the interference fringes resulting from the macroscopic wavefunction of the EC[19]. Within that context, if observed, EC force would pose an alternative evidence for the longly sought condensed state. Throughout this section, we will use the DQW

geometry depicted in Chapter 2.

4.2 Condensation free energy and the emergence of the EC force

It is well known that, a change in the potential energy with respect to distance gives rise to a force. In the case of EC, we are interested in the condensation free energy (CFE), which is a thermodynamic potential as analogues to potential energy in mechanical systems. In our case, there are two contributions to CFE so that $\Omega_\Delta = \Omega_\Delta^{(1)} + \Omega_\Delta^{(2)}$. The first term is the standard free energy term that can be found in any standard text book on statistical mechanics, for instance Greiner's book[50]:

$$\Omega_\Delta^{(1)} = \frac{\partial}{\partial\beta}\sum_{\mathbf{k},\nu} ln[1 - f_\nu(\mathbf{k})] \tag{4.1}$$

The second contribution to CFE arises from the constant term which we neglected previously, coming from the mean field, and is given by $\Omega_\Delta^{(2)} = \sum_{\mathbf{k},\sigma,\sigma'}\langle e^\dagger_{\mathbf{k}',\sigma} h^\dagger_{-\mathbf{k}',\sigma'}\rangle\langle e_{\mathbf{k},\sigma'} h_{\mathbf{k},\sigma}\rangle$. This constant term adds upto the CFE and is purely resultant from the presence of the condensate. Lets derive this term by calculating the thermodynamic averages. We will concentrate on the dark couplings only, since the GS is dominated by those states so bright contribution is negligible. Therefore we will drop the spin dependencies from now on. We can rewrite this term in terms of the EC OP times the remaining term:

$$\Omega_\Delta^{(2)} = \Delta(\mathbf{k})\langle e_\mathbf{k} h_\mathbf{k}\rangle \tag{4.2}$$

The remaining thermodynamic average can be calculated using the unitary transformation that connects the particle-hole basis to the diagonalized quasiparticle basis, which is given by Eq.(3.7). Doing so we have:

$$\Omega_\Delta^{(2)} = \frac{\Delta^2(\mathbf{k})}{2\lambda_{bfk}}\Big[f_1(\mathbf{k}) - f_2(\mathbf{k})\Big] \tag{4.3}$$

which together with Eq.(4.1) yields the total CFE:

$$\Omega_\Delta = \frac{\Delta^2(\mathbf{k})}{2\lambda_{bfk}}\Big[f_1(\mathbf{k}) - f_2(\mathbf{k})\Big] + \frac{\partial}{\partial\beta}\sum_{\mathbf{k},\nu} ln[1 - f_\nu(\mathbf{k})] \tag{4.4}$$

We need change of the free energy in order to calculate the EC force which is given by:

$$\Delta\Omega = \Omega_\Delta - \Omega_N \tag{4.5}$$

where Ω_N is the free energy of the noninteracting case given by $\Omega_N = \frac{\partial}{\partial\beta}\sum_{\mathbf{k},\nu} ln[1-\tilde{f}_\nu(\mathbf{k})]$ with $\tilde{f}_\nu(\mathbf{k})$ being the Fermi-Dirac distributions of the normal state. Now we are in position to express the EC force:

$$\mathcal{F}_{EC} = -\sum_{\mathbf{k}} \frac{\delta\Delta\Omega}{\delta D} = -\sum_{\mathbf{k}} \frac{\delta\Delta\Omega}{\delta\Delta(\mathbf{k})}\frac{\partial\Delta(\mathbf{k})}{\partial D} \tag{4.6}$$

EC force is the direct manifestation of the D-dependence of the EC OP, which is the result of the D-dependence of the Coulomb interaction $v(\mathbf{r}-\mathbf{r}') = e^2/(4\pi\epsilon|\mathbf{r}-\mathbf{r}'-D\mathbf{e}_z|)$.

4.3 Numerical Results

The self consistent set of equations we are solving are exactly the same except this time instead of assuming equal dark-bright pairings, we are only considering the dark OPs $\Delta_{\uparrow\uparrow}(\mathbf{k}) = \Delta_{\downarrow\downarrow}(\mathbf{k}) = \Delta(\mathbf{k})$ and $\Delta_{\uparrow\downarrow}(\mathbf{k}) = \Delta_{\downarrow\uparrow}(\mathbf{k}) = 0$. Fig.(4.1) illustrates the phase boundary of the EC, for the parameter space of layer separation and wavevector. As it can be seen from the figure, the phase boundary is sharp, meaning EC OP drastically diminishes to zero above the critical separation, i.e. $D > D_c$.

4.4 Semi-analytical derivation of the EC force

For a better understanding of the EC force it is instructive to device a method to obtain some analytical results. We will resort to a semi-analytical approach and try to derive the square root dependence of the Δ on the layer separation.

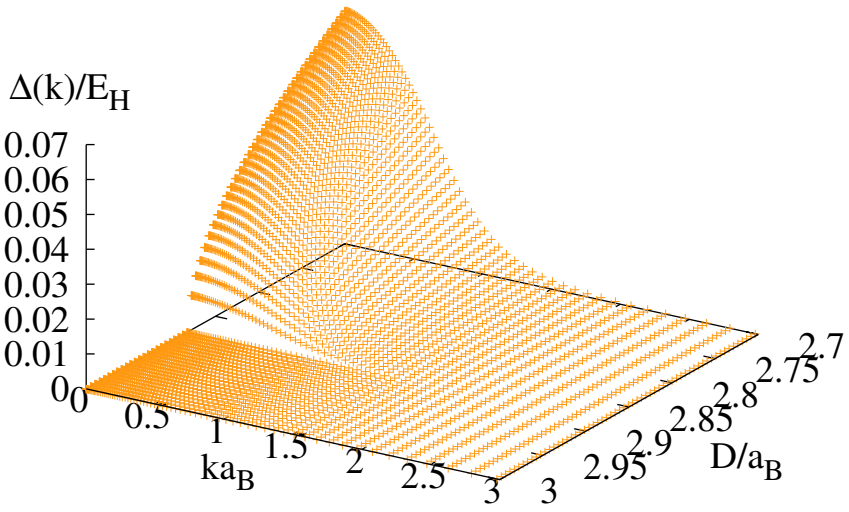

Figure 4.1: The EC OP scaled with Hartree energy versus layer separation D and wavevector k, in units of a_B is plotted for $n^{(+)}a_B^2 = 0.1$. When critical separation is reached, EC OP diminishes to zero rapidly.

4.4.1 Parabolic approximation

We will start with Eq.3.11 and recast it at $T = 0$ in the following form:

$$\Delta(\mathbf{k}) = -\frac{\pi e^2}{\epsilon}\int \frac{\mathbf{dq}}{(2\pi)^2}\frac{e^{-qD}}{q}G_{\mathbf{k+q}}, \qquad G_{\mathbf{k}} = \frac{\Delta(\mathbf{k})F_{\mathbf{k}}}{\sqrt{(\varepsilon_{\mathbf{k}}^{(+)} - \mu_+)^2 + \Delta(\mathbf{k})^2}} \tag{4.7}$$

with,

$$\lim_{k\to 0} F_{\mathbf{k}} = \begin{cases} (1) & \text{if} \quad \Delta^2(0) + \mu_+^2 < \mu_-^2 \\ -1 & \text{if} \quad \Delta^2(0) + \mu_+^2 > \mu_-^2 \end{cases} \tag{4.8}$$

The first case in Eq.(4.8) requires a high electron-hole density mismatch for which Eq.(4.7) has no non-zero solution, whereas second case is consistent with Eq.(4.7). Choosing $\mu_- = 0$ we have the following expression for the exciton density:

$$n^{(+)} = \frac{1}{\mathcal{A}}\sum_{\mathbf{k}}\left[1 - \frac{\varepsilon_{\mathbf{k}}^{(+)}}{\lambda_{\mathbf{k}}}\right] \tag{4.9}$$

It is not possible to solve Eq.(4.7) and Eq.(4.9) analytically due to the momentum dependence of Coulomb potential which also requires a momentum dependent OP.

We will use a parabolic approximation to tackle this problem.Our approximation will be valid for $qD \ll 1$ which gives the leading contribution for the exponential term e^{-qD}. Respecting that condition we can expand $\Delta(\mathbf{k})$ and $G_{\mathbf{k}}$ up to second order, i.e. a parabolic approximation around $q = 0$:

$$G_{\mathbf{k+q}} \simeq G_{\mathbf{k}} + \nabla_{\mathbf{k}} G_{\mathbf{k}} \cdot \mathbf{q} + \frac{q^2}{2} G''_{\mathbf{k}} \tag{4.10}$$

$$\Delta(\mathbf{k}) \simeq \Delta(0) + \nabla_{\mathbf{k}} \Delta(\mathbf{k})|_{k=0} + \frac{k^2}{2} \Delta''(\mathbf{k})|_{k=0} \tag{4.11}$$

At $k = 0$ gap equation becomes:

$$\Delta(0) = -\frac{e^2}{2\epsilon} \int_0^\infty dk \; e^{-kD} G_{\mathbf{k}} \tag{4.12}$$

Performing the integral for $kD \ll 1$,

$$\Delta(0) = -\frac{e^2}{2\epsilon} \Big[\frac{G_0}{D} + \frac{1}{D^3} \left[G''_{\mathbf{k}} \right]|_{k=0} \Big] \tag{4.13}$$

for the sake of simplicity let us choose $\varepsilon_k^{(-)} = 0$. The first derivative of $G_{\mathbf{k}}$ is given by:

$$G'_{\mathbf{k}} = \frac{\lambda_{\mathbf{k}} \Delta'(\mathbf{k}) - \Delta(\mathbf{k}) \lambda'_{\mathbf{k}}}{\lambda^2_{\mathbf{k}}}$$

at $k = 0$ first derivative of $G_{\mathbf{k}}$ is equal to zero. Now lets calculate the second derivative:

$$G''_{\mathbf{k}} = \frac{\lambda_{\mathbf{k}} \Delta''(\mathbf{k}) - \Delta(\mathbf{k}) \lambda''_{\mathbf{k}}}{\lambda^2_{\mathbf{k}}} - \frac{2\lambda'_{\mathbf{k}} [\lambda_{\mathbf{k}} \Delta'(\mathbf{k}) - \Delta(\mathbf{k}) \lambda'_{\mathbf{k}}]}{\lambda^3_{\mathbf{k}}}$$

$$\left[G''_{\mathbf{k}} \right]|_{k=0} = \frac{\lambda_0 \left[\Delta''(\mathbf{k}) \right]|_{k=0} - \Delta(0) \left[\lambda''_{\mathbf{k}} \right]|_{k=0}}{\lambda_0^2}$$

here $[\lambda''_{\mathbf{k}}]|_{k=0}$ is given by:

$$[\lambda''_{\mathbf{k}}]|_{k=0} = \frac{\Delta_0\,[\Delta''(\mathbf{k})]|_{k=0} - \mu_+\hbar^2/m_e^*}{\lambda_0}$$

we also know that zeroth order term in the expansion of $G_{\mathbf{k}}$ is given by:

$$G_0 = -\frac{\Delta(0)}{\lambda_0}$$

Now we can plug G_0 and $[G''_{\mathbf{k}}]|_{k=0}$ in Eq.4.13 which after some rearrangement leads us to the following equation:

$$-\frac{2\Delta(0)\epsilon D^3}{e^2} + \frac{\Delta(0)D^2}{\lambda_0} = \frac{1}{\lambda_0^2}\Big[\lambda_0\Delta''(0) - \Delta(0)\frac{\Delta(0)\Delta''(0) - \mu_+\hbar^2/m_e^*}{\lambda_0}\Big]$$

here we dropped writing $|_{k=0}$ all the time and used a shorthand notation instead, by shortly writing $\Delta''(0)$ for instance.

From the above equation we can write the coefficient of the second order term in the expansion of $\Delta(\mathbf{k})$ as:

$$\Delta''(0) = \left[\frac{\lambda_0}{\lambda_0^2 - \Delta^2(0)}\right]\left(-\frac{2\Delta(0)\lambda_0^2 D^2}{U_c} + \Delta(0)\lambda_0 D^2 - \frac{\Delta(0)\mu_+\hbar^2/m_e^*}{\lambda_0}\right)$$

where $U_c = e^2/\epsilon D$ We can further simplify the above expression by using the fact that $\lambda_0 = U_c/2$ and $\lambda_0^2 - \Delta^2(0) = \mu_+^2$ This will lead us to the simple form given below:

$$\Delta''(0) = -\frac{\Delta(0)\hbar^2}{\mu_+ m_e^*} \tag{4.14}$$

We can find an explicit expression for $\lambda_{\mathbf{k}}$ by using the Taylor expansion of $\Delta(\mathbf{k})$ in $\lambda_{\mathbf{k}} = \sqrt{(\varepsilon_{\mathbf{k}}^{(+)} - \mu_+)^2 + \Delta^2(\mathbf{k})}$ and neglecting the terms of order k^3

$$\lambda_{\mathbf{k}} = \sqrt{(\varepsilon_{\mathbf{k}}^{(+)})^2 + \mu_+^2 - 2\varepsilon_{\mathbf{k}}^{(+)})\mu_+ + \Delta(0)^2 + \frac{[\Delta''(0)]^2 k^4}{4} + \Delta(0)\Delta''(0)k^2}$$

we can have further simplifications if we switch to energy representation by simply invoking $\varepsilon_{\mathbf{k}}^{(+)} = \frac{\hbar^2 k^2}{2m_e^*}$ and writing the expression for $\Delta''(0)$

$$\lambda_{\mathbf{k}} = \sqrt{\Big[(\varepsilon_{\mathbf{k}}^{(+)})^2 - 2\varepsilon_{\mathbf{k}}^{(+)}\mu_+ + \mu_+^2\Big]\Big[1 + \frac{\Delta^2(0)}{\mu_+^2}\Big]}$$

using again the expression $\lambda_0^2 - \Delta^2(0) = \mu_+^2$ and getting rid of the radical we can finally write;

$$\lambda_{\mathbf{k}} = \frac{\lambda_0}{\mu_+}|\varepsilon_{\mathbf{k}}^{(+)} - \mu_+| \tag{4.15}$$

By using the same parabolic approximation in Eq.(4.9) we have:

$$\mu_+ = -\frac{\lambda_0}{2} + \sqrt{\left(\frac{\lambda_0}{2}\right)^2 + \frac{\lambda_0 n_+}{\Gamma}} \tag{4.16}$$

where $\Gamma = m_e^*/(2\pi\hbar^2)$ is the 2D density of states. After deriving these relations, we can now show the desired square root relation of the EC OP:

$$\Delta(0) \simeq \sqrt{\frac{4}{3}}\lambda_0\sqrt{1 - \frac{D}{D_c}} \tag{4.17}$$

where $D_c = e^2/(2\epsilon\mu_+)$. Moreover, we can use Eq.(4.5) to derive a similar result for the free energy:

$$\Delta\Omega = -3\Gamma\mu_0^2\left(1 - \frac{D}{D_c}\right) \tag{4.18}$$

Eq.(4.17) and Eq.(4.18) shows the success of our model in generating the basic features of the numerical calculations of the previous section. The comparison of

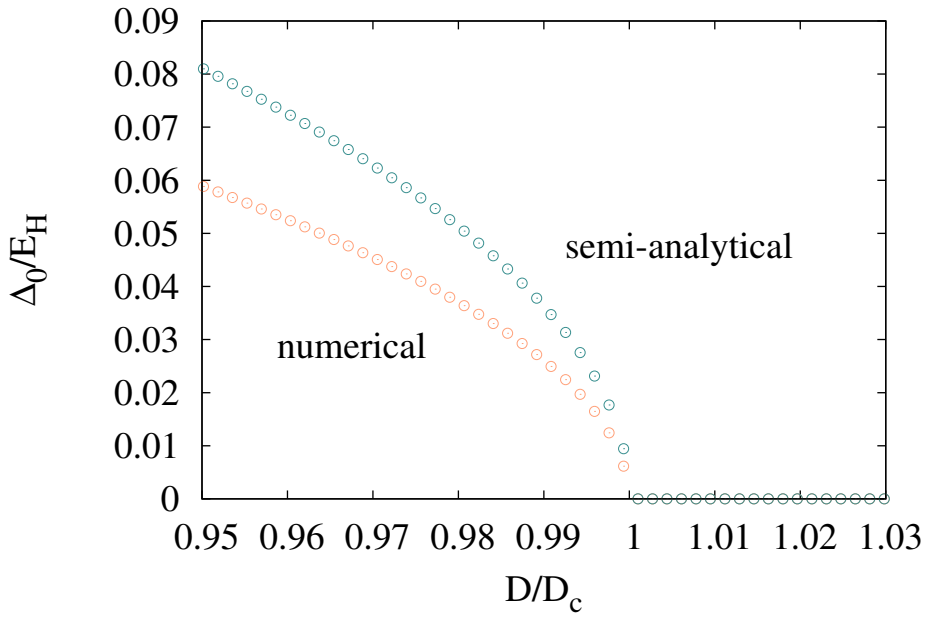

Figure 4.2: The EC OP at $k = 0$ scaled with E_H as a function of the dimensionless layer separation D/a_B is plotted using the numerical and semi-analytical calculations. The results show the success of the parabolic approximation in generating the square root behavior of $\Delta(0)$ with increasing layer separation.

these equations with numerical results are given in Fig. 4.2 and Fig. 4.3. The main result of our parabolic approximation is the estimation of the force, which can be written using the above relations obtained from the parabolic approximation in Eq.(4.6):

$$\frac{\mathcal{F}_{EC}}{\mathcal{A}} \simeq -\frac{3}{4}\frac{[n^{(+)}]^2}{\Gamma D_c} \tag{4.19}$$

For a concentration of $n^{(+)} \simeq 3 \times 10^{11} cm^{-2}$ and an area of $\mathcal{A} \simeq 10^3 \mu m^2$ the EC force is estimated to be $\mathcal{F}_{EC} \simeq 10^{-9} N$.

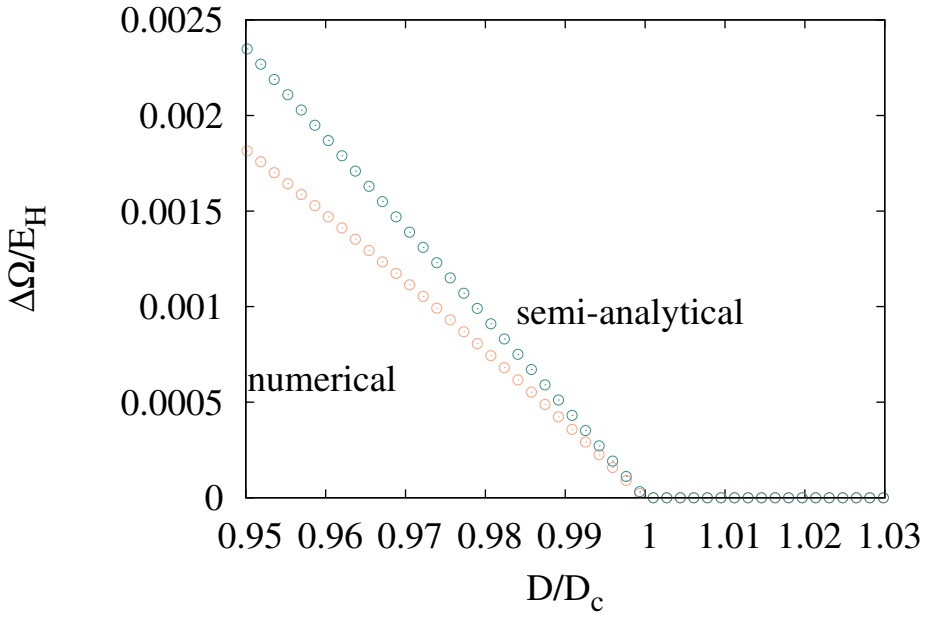

Figure 4.3: Change of the free energy scaled with the E_H as a function of the dimensionless layer separation D/a_B is plotted using the numerical and semi-analytical calculations. Again the power of the parabolic approximation can be seen from the comparison of numerical and semi-analytical results.

Chapter 5

EC-CDW Instability Competition and EC-Force in TMDC

5.1 Introduction

Theoretical studies on the coexisting conventional superconductivity (CSC) and charge density wave (CDW) instability orders in 1D systems were reported in mid 70's[51, 52]. The 2D extension of these competing orders was demonstrated by Balseiro and Falicov[53]. After the stimulating discussions with Vladimir Yudson, we made studies on the coexisting EC-CDW states, in order to enhance the EC force discussed in the previous chapter. Since both EC and CDW couplings are much stronger in transition metal dichalcogenides (TMDC) accompanied by high transition temperatures $T_c^{EC} \simeq T_c^{CDW} \simeq 100K$. The CDW and CSC states were speculated to coexist in TDMCs[54]. A detailed compilation of the theory and experiment on coexisting CDW-CSC states in TDMCs can be found in the review by Gabovich *et al.*[55].

We will investigate EC and EC force in 1T-$TiSe_2$ structure in this chapter. 1T-$TiSe_2$ is a layered TMDC, consisting of a Titanium layer sandwiched between two Selenium layers. The Se-Ti-Se layers are periodically repeated, forming the 1T-$TiSe_2$ structure. An interesting feature of this layered structure is the observation of the superlattice formation[56, 57]. The microscopic theory appeared later[58] but the mechanism behind the periodic lattice distortions is still controversial. Out of many, three scenarios are on debate: a) Fermi surface (FS) nesting, b) band Jahn-Teller effect, c) excitonic condensation. The latter two are stronger candidates with experimental support[59, 60, 61]. More recent results makes the third scenario to be the strongest candidate[62, 63, 64] accompanied by high T_c^{EC} values.

We will not only demonstrate the emergence of the EC force in this chapter, but we will also speculate that, our model can pose an alternative scenario for the periodic lattice distortions in 1T-$TiSe_2$. Moreover we will show that the two transition temperatures of CDW and EC orders, T_c^{CDW} and T_c^{EC} can be tuned by changing the electron-phonon coupling constant λ_{ep}[65].

5.2 Theory of CDW Instability

5.2.1 CDW Instability in 1D Systems

CDW instability is well understood in 1D, quasi-1D or more generally low-dimensional systems. The nomenclature used here mainly refers to the crystal and electronic structure of the materials, since real-life 1D materials are quite rare and the theory we are going to present is safely applicable to these systems.

The response to an external potential is well understood within the context of linear response theory. We will follow the strategy used by Grüner [66] Lets assume that we have a potential V which will cause the re-distribution of the charges in our system. The induced charge distribution can be expressed in terms of the potential V using the Lindhard response function (also called the

linear susceptibility function):

$$\rho_{ind}(q) = \chi(q)V(q) \tag{5.1}$$

1D expression given above is the special case of the d-dimensional case. Linear susceptibility function is given by:

$$\chi(q) = \int \frac{dk}{2\pi} \frac{f(k) - f(k+q)}{\varepsilon_k - \varepsilon_{k+q}} \tag{5.2}$$

where $f(k)$ is the Fermi-Dirac function and ε_k is the energy dispersion relation. In a 1D system, Fermi surface consists of two points, one at k_F and other at $-k_F$, k_F being the Fermi wave vector. When these two points of the Fermi surface, separated by $q = 2k_F$ is connected (nomenclature for this process is *nesting* and moreover for this special 1D case it is referred as *perfect nesting*) by the wavevector $q = 2k_F$, the linear susceptibility function diverges, indicating an instability. Before studying the 1D case in detail let us first briefly compare the response function in 1D, 2D and 3D.

A detailed derivation of response functions for one, two and three dimensional cases are presented in Mihaila's preprint[67]. To be more precise, we are talking about the static response function, which is defined as the negative of the Lindhard function with zero energy:

$$F(\mathbf{q}) = -\chi(\mathbf{q}, \omega = 0) \tag{5.3}$$

Their behaviour at $q = 2k_F$ are the same so we are safe to use the static response function instead of the full Lindhard function. For the static response functions in 1D, 2D, and 3D respectively, we have the following expressions:

$$\begin{aligned} F_1(u) &= \frac{N_1}{2u\varepsilon_F} ln\left|\frac{1+u/2}{1-u/2}\right| \\ F_2(u) &= \frac{N_2}{\varepsilon_F}\left[1 - \Theta(u-2)\sqrt{1-(2/u)^2}\right] \\ F_3(u) &= \frac{3N_3}{4\varepsilon_F}\left[1 + \frac{1-(u/2)^2}{u} ln\left|\frac{1+u/2}{1-u/2}\right|\right] \end{aligned} \tag{5.4}$$

where $\varepsilon_F = \hbar^2 k_F^2/2m$ is the Fermi energy, Θ denotes the Heaviside step function, $u = q/k_F$ is the rescaled wavevector and N_d $(d = 1, 2, 3)$ is the density particle

density defined by:

$$N_d = 2 \int_{k \leq k_F} \frac{d^d k}{(2\pi)^d} \tag{5.5}$$

As we already pointed out, response function diverges at $q = 2k_F$ for the 1D

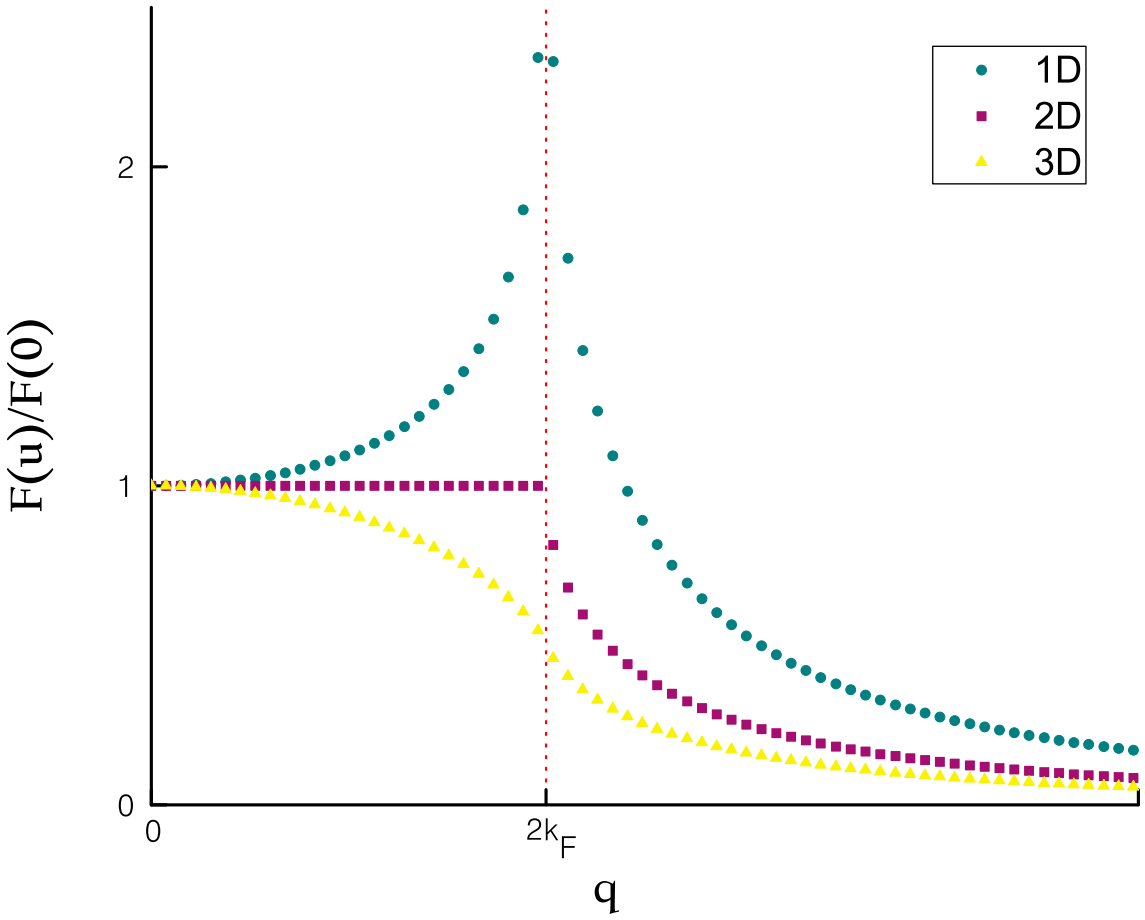

Figure 5.1: The static response functions versus the dimensionless wave vectors plotted for 1D, 2D and 3D.

case. For the two- and three- dimensional cases the response function does not diverge at $q = 2k_F$, instead its derivative has a a singularity. This result makes 1D case much more significant. Let us first move on with the 1D case, then we will extend these ideas to the two dimensional case to serve our purposes.

We have seen that the external potential will result in an induced charge distribution. Going one step forward, this induced charge distribution will also induce a potential. Lets assume the following form for the this induced potential:

$$V_{ind}(q) = -\tilde{\lambda}\rho_{ind}(q) \tag{5.6}$$

where $\tilde{\lambda}$ is a wavevector-independent coupling constant, which in our case results from the electron-phonon coupling that we will study below. Writing the total potential in terms of the induced and the external potentials, $V = V_{ext} + V_{ind}$ and combining this expression, Eq.(5.2). and Eq.(5.6)., we have:

$$\rho_{ind}(q) = \frac{\chi(q)V_{ext}(q)}{1 + \tilde{\lambda}\chi(q)} \tag{5.7}$$

A quick look at the above equation suggests that for a negative coupling constant i.e., an attractive interaction, we can have a divergent charge distribution, hence an instability.

Let us also present the microscopic origin of this attractive interaction. The interaction of electrons with the lattice, i.e phonons is well described by Fröhlich [68]. The so called Fröhlich Hamiltonian consists of three terms. Electronic part, ionic part, and the part that describes the electron-phonon interaction:

$$H = H_{el} + H_{lat} + H_{ep} \tag{5.8}$$

with individual terms given as:

$$\begin{aligned} H_{el} &= \sum_k \varepsilon_k e_k^\dagger e_k \\ H_{lat} &= \sum_q \hbar w_q [1/2 + a_q^\dagger a_q] \\ H_{int} &= \sum_{k,q} \tilde{\lambda}_q e_{k+q}^\dagger e_k [a_q + a_{-q}^\dagger] \end{aligned}$$

So the full Hamiltonian reads:

$$H = \sum_k \varepsilon_k e_k^\dagger e_k + \sum_q \hbar w_q (1/2 + a_q^\dagger a_q) + \sum_{k,q} \tilde{\lambda}_q e_{k+q}^\dagger e_k [a_q + a_{-q}^\dagger] \tag{5.9}$$

5.2.2 Microscopic Theory of CDW for 2D Systems

Before starting to adopt the 1D theory to the 2D case, we should first remember that dimensionality drastically affects the CDW formation; in the 1D case we have perfect nesting, where two points of the Fermi surface are exactly connected by the nesting wavevector $\mathbf{Q}$. On the other hand, in its higher dimensional counterparts, apart from some special cases, we cannot really talk about perfect nesting.

A microscopic theory for analyzing coexisting CDW and SC states in two-dimensional systems was presented in late 70's[53]. We will borrow the ideas from that manuscript and replace SC with EC to serve our purposes and moreover extend the formalism to a layered system. Lets begin by recasting the Hamiltonian defined in Eq.(5.8). by extending it to 2D in the following way:

$$H_{CDW} = H_{el} + H_{int}^{CDW} \tag{5.10}$$

where the interaction(spin degree of freedom is traced out since otherwise we will end up with an 8×8 Hamiltonian whose eigeneneriges and eigenfunctions are hard if not impossible to find analytically and moreover spin dependent calculations are out of the scope of this work) responsible for the CDW instability reads:

$$H_{int}^{CDW} = \frac{1}{4}\sum_{\mathbf{k},\mathbf{k}'}[V_{\mathbf{kQ}} + V_{\mathbf{k}'\mathbf{Q}}]e^{\dagger}_{\mathbf{k}+\mathbf{Q}}e^{\dagger}_{\mathbf{k}'+\mathbf{Q}}e_{\mathbf{k}'}e_{\mathbf{k}} \tag{5.11}$$

In the above equation, $\mathbf{Q}$ is our nesting vector(in this formalism we are limiting ourselves to a single wave vector, which in the ideal case is not true for 2D systems, but this limitation is safely acceptable within the context of our formalism since we will also assume perfect nesting by fixing the chemical potential to zero and also neglecting the distortions in the Fermi surface in nesting wavevector related calculations) satisfying $\mathbf{k} + 2\mathbf{Q} = \mathbf{k}$, which means we are choosing a nesting vector that is commensurate with the underlying lattice and $V_{\mathbf{kQ}}$ is the wave vector-dependent electron-phonon interaction given by:

$$V_{\mathbf{kQ}} = \frac{2\tilde{\lambda}^2\hbar\omega_{\mathbf{Q}}}{[\varepsilon_{\mathbf{k}} - \varepsilon_{\mathbf{k}+\mathbf{Q}}]^2 - [\hbar\omega_{\mathbf{Q}}]^2} \tag{5.12}$$

At this step, we can assume a BCS-like[29] momentum-independent form so that the electron-phonon interaction becomes just a simple constant:

$$V_{\mathbf{kQ}}^{CDW} = \begin{cases} -\lambda, & \text{if} \quad |\varepsilon_{\mathbf{k}} - \mu| < \hbar\omega_D \ \& \ |\varepsilon_{\mathbf{k+Q}} - \mu| < \hbar\omega_D, \\ 0, & \text{otherwise} \end{cases} \tag{5.13}$$

where μ is the chemical potential and $\hbar\omega_D$ is the Debye energy. We can now use mean-field approximation in Eq.(5.11).to obtain:

$$H_{int}^{CDW} = -G_0 \sum_{\mathbf{k}} e_{\mathbf{k+Q}}^{\dagger} e_{\mathbf{k}} - G_1 \sum_{\mathbf{k}}'' e_{\mathbf{k+Q}}^{\dagger} e_{\mathbf{k}} + G_0 G_1/\lambda \tag{5.14}$$

In the above equations double primed sums are performed only when $|\varepsilon_{\mathbf{k}} - \mu| < \hbar\omega_D$ and $|\varepsilon_{\mathbf{k+Q}} - \mu| < \hbar\omega_D$, with CDW order parameter $G_{\mathbf{k}}$ defined in the following manner:

$$\begin{aligned} G_{\mathbf{k}} &= \begin{cases} G_0 + G_1 & \text{if} \quad |\varepsilon_{\mathbf{k}} - \mu| < \hbar\omega_D \ , \\ G_0, & \text{otherwise} \end{cases} \\ G_0 &\equiv \sum_{\mathbf{k}}'' \langle e_{\mathbf{k+Q}}^{\dagger} e_{\mathbf{k}} \rangle \\ G_1 &\equiv \sum_{\mathbf{k}} \langle e_{\mathbf{k+Q}}^{\dagger} e_{\mathbf{k}} \rangle \end{aligned} \tag{5.15}$$

5.3 A model for CDW and EC orders in layered systems

After laying the basics of the CDW instability in 2D, we are now in a position to present the competition of CDW and EC orders. We will extend the theory used by Balseiro and Falicov[53] for explaining the CSC/CDW competition to investigate the competing orders of EC/CDW in layered systems. We will start with two layers, with strong Fermi surface (FS) nesting giving rise to separate CDWs in separate layers. For each layer, we assume a square lattice with a lattice constant $a = 5\mathring{A}$. We will use a tight binding approach in which the interlayer hoppings are neglected, i.e. only intralayer hoppings are considered. Furthermore, the two layers are coupled by the short range Coulomb attraction. Due to the strong electronic repulsion, those two CDW layers have a relative π-shift:

$$\langle \hat{\rho}_u(\mathbf{r}) \rangle = n_0 + \gamma_u n_1 cos(\mathbf{Q} \cdot \mathbf{r}) \tag{5.16}$$

in which $\hat{\rho}_u(\mathbf{r}) = \hat{u}^\dagger(\mathbf{r})\hat{u}(\mathbf{r})$ denotes the density operator of the upper layer with $\hat{u}^\dagger(\mathbf{r})/\hat{u}(\mathbf{r})$ being creation/annihilation operators in real space, n_0 is the mean density, n_1 is the CDW order amplitude, $\mathbf{Q} = (\pi, \pi)$ is the nesting vector satisfying $\mathbf{k} + 2\mathbf{Q} = \mathbf{k}$ and $\gamma_u = 1$. For the down layer $\hat{d}^\dagger(\mathbf{r})/\hat{d}(\mathbf{r})$ replace $\hat{u}^\dagger(\mathbf{r})/\hat{u}(\mathbf{r})$ and $\gamma_d = -1$. We can write the Coulomb interaction via the density operators:

$$\hat{v}_{int} = \int d\mathbf{r}d\mathbf{r}'\hat{\rho}_u(\mathbf{r})V(\mathbf{r}-\mathbf{r}')\hat{\rho}_d(\mathbf{r}') \tag{5.17}$$

where $V(\mathbf{r}-\mathbf{r}') = e^2/(4\pi\epsilon|\mathbf{r}-\mathbf{r}'-D\mathbf{e}_z|)$ is the Coulomb interaction in real space with ϵ, e, $\mathbf{e}_z$ and D are the dielectric constant, electron charge, unit vector in z-direction and layer separation respectively. Ground state average of Eq.(5.17) yields three terms: a) a term proportional to n_0^2 b) a term proportional to n_1^2 and c) two other terms first order in n_0 canceling each other:

$$\langle\hat{v}_{int}\rangle = \int d\mathbf{r}d\mathbf{r}'V(\mathbf{r}-\mathbf{r}')[n_0^2 - \tilde{n}_1(\mathbf{r})\tilde{n}_1(\mathbf{r}')] \tag{5.18}$$

with $\tilde{n}_1(\mathbf{r}) = n_1 cos(\mathbf{Q}\cdot\mathbf{r})$. The first term can be absorbed into the chemical potential since it is a constant and the second term is attractive resultant from the π-shift. When n_1 is nonzero, two layers are couple as electron-hole layers. The dispersion of the square lattice we use in our model is given by:

$$\epsilon_{\mathbf{k}} = -2t_0[cos(k_x a) + cos(k_y a)] - 4t_1 cos(k_x a)cos(k_y a) \tag{5.19}$$

here t_0 and t_1 are the first and second nearest neighbour (NN) interaction strengths respectively. Considering the nesting, the important correlations are the following[53]:

$$n_0 = [1/(2\pi)^2]\int \mathbf{dk}\langle\hat{u}^\dagger_{\mathbf{k}}\hat{u}_{\mathbf{k}}\rangle, \qquad n_1 = G/2\lambda_{ep} \tag{5.20}$$

in which λ_{ep} denotes the momentum-independent electron-phonon interaction coupling strength, just as depicted in Eq.(5.13). This time we have the 2D extended version of Eq.(5.15) with the same definition of G:

$$G_0 = \lambda_{ep}\int'' \frac{\mathbf{dk}}{(2\pi)^2}\langle\hat{u}^\dagger_{\mathbf{k}}\hat{u}_{\mathbf{k}+\mathbf{Q}}\rangle \qquad \text{and} \tag{5.21}$$

$$G_1 = \lambda_{ep}\int \frac{\mathbf{dk}}{(2\pi)^2}\langle\hat{u}^\dagger_{\mathbf{k}}\hat{u}_{\mathbf{k}+\mathbf{Q}}\rangle \tag{5.22}$$

with the following self consistency conditions:$\langle\hat{u}^\dagger_{\mathbf{k}}\hat{u}_{\mathbf{k}}\rangle = \langle\hat{d}^\dagger_{\mathbf{k}}\hat{d}_{\mathbf{k}}\rangle$ and $\langle\hat{u}^\dagger_{\mathbf{k}}\hat{u}_{\mathbf{k}+\mathbf{Q}}\rangle = -\langle\hat{d}^\dagger_{\mathbf{k}}\hat{d}_{\mathbf{k}+\mathbf{Q}}\rangle$. The first condition is due to our choice of identical layers with same

particle densities and second condition arises as a result of the π-shift. Now we can present our Hamiltonian after the Hartree-Fock mean field approximation in the $(\hat{u}^\dagger_{\mathbf{k}}\,\hat{u}^\dagger_{\mathbf{k+Q}}\,\hat{d}^\dagger_{\mathbf{k}}\hat{d}^\dagger_{\mathbf{k+Q}})$ basis as:

$$\mathcal{H} = \sum_{\mathbf{k}} \left\{ H_0 + \begin{pmatrix} \epsilon^{(-)}_{\mathbf{k}} & -G & \Delta^{(1)}_{\mathbf{k}} & \Delta^{(2)}_{\mathbf{k}} \\ -G & -\epsilon^{(-)}_{\mathbf{k}} & \Delta^{(2)}_{\mathbf{k}} & \Delta^{(1)}_{\mathbf{k+Q}} \\ \Delta^{(1)}_{\mathbf{k}} & \Delta^{(2)}_{\mathbf{k}} & \epsilon^{(-)}_{\mathbf{k}} & G \\ \Delta^{(2)}_{\mathbf{k}} & \Delta^{(1)}_{\mathbf{k+Q}} & G & -\epsilon^{(-)}_{\mathbf{k}} \end{pmatrix} \right\} \tag{5.23}$$

in which the spin is eliminated due to degeneracy, $H_0 = (\epsilon^{(+)}_{\mathbf{k}} - \mu)\sigma_{\mathbf{0}} \otimes \sigma_{\mathbf{0}}$, $\epsilon^{(+)}_{\mathbf{k}} = (\epsilon_{\mathbf{k}} + \epsilon_{\mathbf{k+Q}})/2$, $\epsilon^{(-)}_{\mathbf{k}} = (\epsilon_{\mathbf{k}} - \epsilon_{\mathbf{k+Q}})/2$ and σ_0 is the 2×2 unit matrix. We have two different momentum dependent pairings in our Hamiltonian, $\langle \hat{u}^\dagger_{\mathbf{k}}\,\hat{d}_{\mathbf{k}} \rangle$ and $\langle \hat{u}^\dagger_{\mathbf{k}}\,\hat{d}_{\mathbf{k+Q}} \rangle$, denoted by $\Delta^{(1)}_{\mathbf{k}}$ and $\Delta^{(2)}_{\mathbf{k}}$ respectively. The ground state is dominated by the latter one in the absence of CDW ordering, so we will deal with the case where $\Delta^{(2)}_{\mathbf{k}} \neq 0$ and $\Delta^{(1)}_{\mathbf{k}} = \Delta^{(1)}_{\mathbf{k+Q}} = 0$ and also for the sake of notation we will redefine $\Delta^{(2)}_{\mathbf{k}}$ as $\Delta_{\mathbf{k}}$. After those clarifications we can diagonalize the Hamiltonian to find the eigenspectrum. The diagonalizing transformation reads:

$$\hat{U} = \frac{1}{\sqrt{2\Lambda(\Lambda - \epsilon^{(-)}_{\mathbf{k}})}} \begin{pmatrix} \Delta_{\mathbf{k}} & 0 & -G & (\Lambda - \epsilon^{(-)}_{\mathbf{k}}) \\ 0 & \Delta_{\mathbf{k}} & -(\Lambda - \epsilon^{(-)}_{\mathbf{k}}) & -G \\ G & (\Lambda - \epsilon^{(-)}_{\mathbf{k}}) & \Delta_{\mathbf{k}} & 0 \\ -(\Lambda - \epsilon^{(-)}_{\mathbf{k}}) & G & 0 & \Delta_{\mathbf{k}} \end{pmatrix} \tag{5.24}$$

which yields a two-fold degenerate eigenspectrum, $E_1 = E_0 + \Lambda$, $E_2 = E_0 - \Lambda$ with $E_0 = \epsilon^{(+)}_{\mathbf{k}} - \mu$ and $\Lambda = [(\epsilon^{(-)}_{\mathbf{k}})^2 + \Delta^2_{hyb}]^{1/2}$ in which $\Delta_{hyb} = (G^2 + \Delta^2_{\mathbf{k}})^{1/2}$ is the hybrid gap. The basis in which the Hamiltonian is diagonal is connected to the old basis via the unitary transformation as given by:

$$\begin{pmatrix} g_{1\mathbf{k}} \\ g_{2\mathbf{k}} \\ g_{3\mathbf{k}} \\ g_{4\mathbf{k}} \end{pmatrix} = \alpha \begin{pmatrix} \Delta_{\mathbf{k}} & 0 & -G & (\Lambda - \epsilon^{(-)}_{\mathbf{k}}) \\ 0 & \Delta_{\mathbf{k}} & -(\Lambda - \epsilon^{(-)}_{\mathbf{k}}) & -G \\ G & (\Lambda - \epsilon^{(-)}_{\mathbf{k}}) & \Delta_{\mathbf{k}} & 0 \\ -(\Lambda - \epsilon^{(-)}_{\mathbf{k}}) & G & 0 & \Delta_{\mathbf{k}} \end{pmatrix} \begin{pmatrix} \hat{u}_{\mathbf{k}} \\ \hat{u}_{\mathbf{k+Q}} \\ \hat{d}_{\mathbf{k}} \\ \hat{d}_{\mathbf{k+Q}} \end{pmatrix}$$

or we can invert the above equation by multiplying both sides by $\hat{U}^\dagger$ from the left to obtain:

$$\begin{pmatrix} \hat{u}_{\mathbf{k}} \\ \hat{u}_{\mathbf{k+Q}} \\ \hat{d}_{\mathbf{k}} \\ \hat{d}_{\mathbf{k+Q}} \end{pmatrix} = \alpha \begin{pmatrix} \Delta_{\mathbf{k}} & 0 & G & -(\Lambda - \epsilon^{(-)}_{\mathbf{k}}) \\ 0 & \Delta_{\mathbf{k}} & (\Lambda - \epsilon^{(-)}_{\mathbf{k}}) & G \\ -G & -(\Lambda - \epsilon^{(-)}_{\mathbf{k}}) & \Delta_{\mathbf{k}} & 0 \\ (\Lambda - \epsilon^{(-)}_{\mathbf{k}}) & -G & 0 & \Delta_{\mathbf{k}} \end{pmatrix} \begin{pmatrix} g_{1\mathbf{k}} \\ g_{2\mathbf{k}} \\ g_{3\mathbf{k}} \\ g_{4\mathbf{k}} \end{pmatrix}$$

where $\alpha = 1/\sqrt{2\Lambda(\Lambda - \epsilon_{\mathbf{k}}^{(-)})}$. We can re-write the above equation in the open form as:

$$\begin{aligned}
\hat{u}_{\mathbf{k}} &= \alpha[\Delta_{\mathbf{k}} g_{1\mathbf{k}} + G g_{3\mathbf{k}} - (\Lambda - \epsilon_{\mathbf{k}}^{(-)}) g_{4\mathbf{k}}] \\
\hat{u}_{\mathbf{k+Q}} &= \alpha[\Delta_{\mathbf{k}} g_{2\mathbf{k}} + (\Lambda - \epsilon_{\mathbf{k}}^{(-)}) g_{3\mathbf{k}} + G g_{4\mathbf{k}}] \\
\hat{u}_{\mathbf{k}} &= \alpha[\Delta_{\mathbf{k}} g_{1\mathbf{k}} + G g_{3\mathbf{k}} - (\Lambda - \epsilon_{\mathbf{k}}^{(-)}) g_{4\mathbf{k}}] \\
\hat{d}_{\mathbf{k+Q}} &= \alpha[(\Lambda - \epsilon_{\mathbf{k}}^{(-)}) g_{1\mathbf{k}} - G g_{2\mathbf{k}} + \Delta_{\mathbf{k}} g_{4\mathbf{k}}]
\end{aligned}$$

Using the above expressions we can cast the final expressions for the OP and number conservation equations:

$$G_0 = -\lambda_{ep}(G_0 + G_1) \int'' \frac{\mathbf{dk}}{(2\pi)^2} \frac{F(\mathbf{k})}{2\Lambda} \tag{5.25}$$

$$G_1 = -\lambda_{ep} \int \frac{\mathbf{dk}}{(2\pi)^2} \frac{G}{2\Lambda} F(\mathbf{k}) \tag{5.26}$$

$$\Delta_{\mathbf{k}} = -\frac{1}{2} \int \frac{\mathbf{dk'}}{(2\pi)^2} \frac{e^2}{2\varepsilon} \frac{e^{-|\mathbf{k}-\mathbf{k'}|D}}{|\mathbf{k}-\mathbf{k'}|} \frac{\Delta_{\mathbf{k'}}}{2\Lambda} F(\mathbf{k'}) \tag{5.27}$$

$$n_0 = \frac{1}{2} \int \frac{\mathbf{dk}}{(2\pi)^2} \Big[\frac{(\Lambda + \epsilon_{\mathbf{k}}^{(-)})}{\Lambda} f_1(\mathbf{k}) + \frac{(\Lambda - \epsilon_{\mathbf{k}}^{(-)})}{\Lambda} f_2(\mathbf{k}) \Big] \tag{5.28}$$

where $F(\mathbf{k}) = f_1(\mathbf{k}) - f_2(\mathbf{k})$, $f_1(\mathbf{k})$ and $f_2(\mathbf{k})$ are the Fermi-Dirac distributions corresponding to E_1 and E_2. Above equations forms a self-consistent set, which we solved numerically. The results are shown in the following section.

Before advancing to the next section, let us demonstrate the form of free energy in this system, which we will use to calculate the EC force similar to the previous chapter. Our starting point is again Eq.(4.6), but this time we have two OPs so we cannot use the second part of that equation, hence sticking to the first part of the equation, we need $\Delta\Omega = \Omega_0 - \Omega_N$ given by:

$$\Omega_O = -A \frac{G_0 G_1}{\lambda_{ep}} + \sum_{\mathbf{k}} \Big[\frac{\Delta_{\mathbf{k}}^2}{2\Lambda} F(\mathbf{k}) + \frac{\partial}{\partial \beta} \sum_{\nu} ln(1 - f_{\nu}(\mathbf{k})) \Big] \tag{5.29}$$

$$\Omega_N = \frac{\partial}{\partial \beta} \sum_{\mathbf{k},\nu} ln(1 - f_{\nu\,0}(\mathbf{k})) \tag{5.30}$$

in which $f_{\nu\,0}(\mathbf{k})$ is the Fermi-Dirac distribution when $\Delta_{\mathbf{k}} = G = 0$. So after calculating the above free energies we can easily calculate the EC force using Eq.(4.6). Let us conclude this section by illustrating a simple scheme to calculate

the periodic lattice distortions that will arise due to the EC force. We can estimate the magnitude of the strain by using the axial stiffness constant $k = AE/L$ as:

$$\Delta x = \frac{\mathcal{F}_{EC}}{k} = \frac{\mathcal{F}_{EC} L}{AE} \tag{5.31}$$

In the above equation the elastic properties arising from the *Ti-lattice-Se* coupling is represented by k, where L is the *Ti-Se* separation, which in our case corresponds to the layer separation D, A is the cross-section area and E is the Young's modulus.

5.4 Results

5.4.1 Competition of EC and CDW instability

The signature of FS nesting on the EC OP can be seen from Fig.(5.2): Firstly, the maxima of the EC OP is connected by the nesting wavevector $\mathbf{Q} = (\pm\pi, \pm\pi)$. Secondly, the maxima of the EC OP shifts from the saddle points $k_{sp} = (0, \pm\pi)$ and $k_{sp} = (\pm\pi, 0)$ to the origin as the second nearest neighbour interaction t_1 increases.

The competition of EC and CDW orders are illustrated in Fig.(5.3). Maximum of the EC order parameter $\Delta_{\mathbf{k}}$ and CDW OP are shown via a color map in which the inverse tangent transformation $f_{col} = tan^{-1}[\frac{\Delta_{max}}{G}]$ is used to present the relative strength of the OPs.

Another significant result is the different configurations obtained via changing second NN interaction strength. Two different configurations together with the phase diagram are demonstrated in Fig.(5.4): i) For large values of t_1 the emergence of CDW instantly destroys EC, so that they don't coexist at all in that regime (Fig. 5.4d). ii) For zero or small values of t_1, as λ_{ep} reaches the critical value, the emergence of CDW instability lowers the EC OP until completely destroying it (Fig. 5.4b, c)

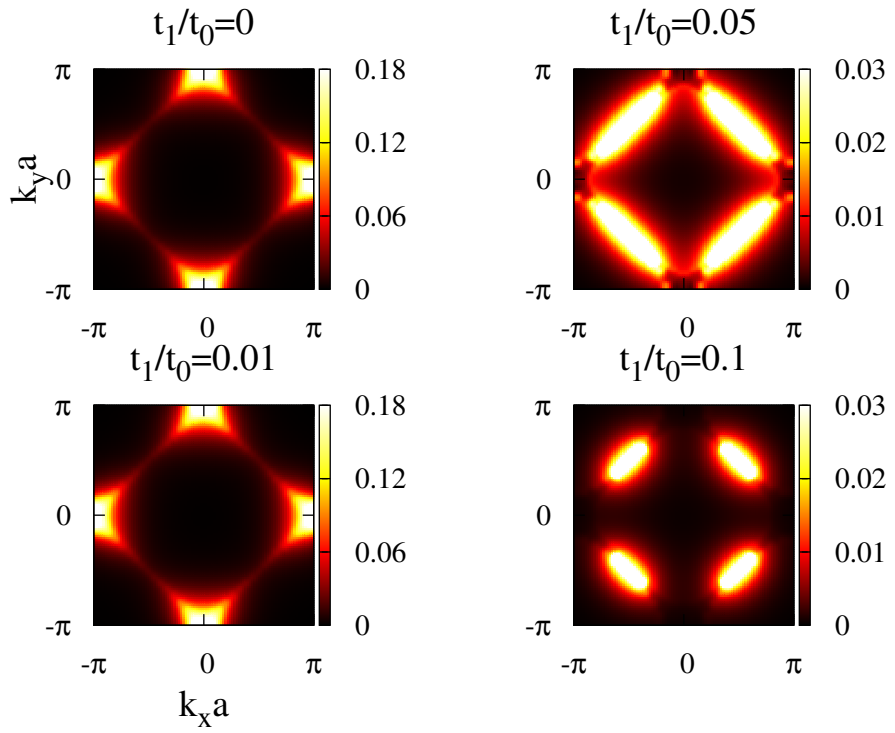

Figure 5.2: EC OP, scaled with $t_0 = 0.125eV$, is plotted for different second NN interaction strengths. The peak positions of the EC OP are separated by the nesting vector, $\mathbf{Q} = (\pm\pi, \pm\pi)$ in each of the four cases. For zero or a small second NN interaction, OP is maximum at the saddle points of the dispersion, due to nearly perfect nesting. As the second NN interaction increases, the perfect nesting gradually disappears.

5.4.2 EC-Force in TMDC

The possibility of the electron-hole coupling in the periodic lattice distortions in $1T\text{-}TiSe_2$ and the presence of strong excitonic background was suggested experimentally by Di Salvo *et al.*[57]. Based on this experimental work, Monney *et*

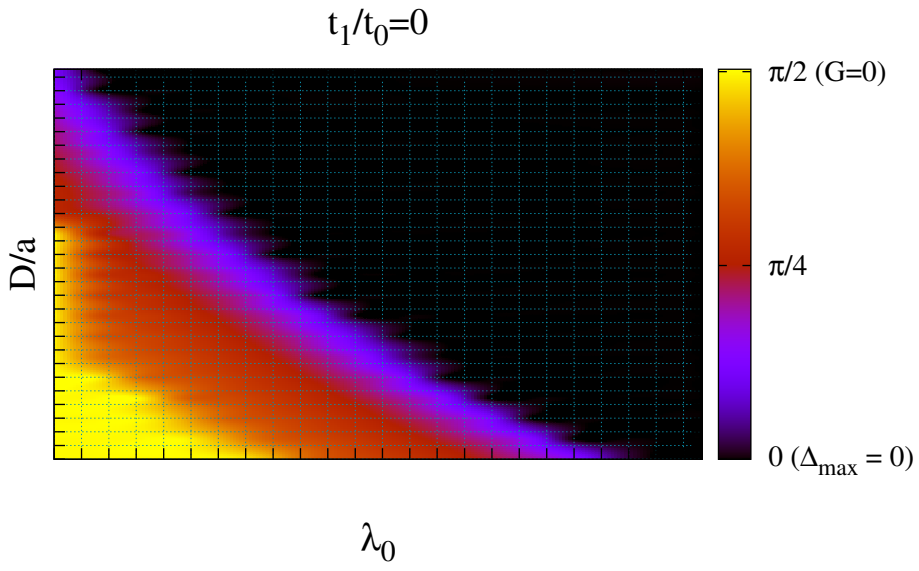

Figure 5.3: Color map of the CDW and EC for $t_1 = 0$. The OPs are mapped via $f_{col} = tan^{-1}[\frac{\Delta_{max}}{G}]$ transformation. In yellow (light) regions there is only EC and in black (dark) regions only CDW is present, whereas in between they coexist. Here, λ_0 runs from 0.9 to 1.6 and D/a varies between 2 and 4.

al., proposed an exciton-phonon coupling based mechanism to explain the lattice distortion[64]. On the other hand, the model we use with two different mechanisms and two different order parameters coupled self consistently is a promising model that can explain the three distinct cases of $T_c^{CDW} < T_c^{EC}, T_c^{CDW} > T_c^{EC}$ and $T_c^{CDW} = T_c^{EC}$. The change of free energy with respect to the layer separation is plotted in Fig.(5.5) for different t_1/t_0 and λ_0 values. There is a significant difference compared to the case we discussed in the previous chapter: In the previous case of GaAs DQWs, the change of free energy is maximum at the phase boundary, i.e. the EC force has its maximum amplitude close to the phase boundary. In the current case of $1T\text{-}TiSe_2$, it is just the opposite. The change of free energy or in other words the EC force is minimum at the phase boundary due to the presence of CDW order and it gets stronger as D moves away from the critical layer separation D_c.

Now we can present one of the main results of this section: We calculated the

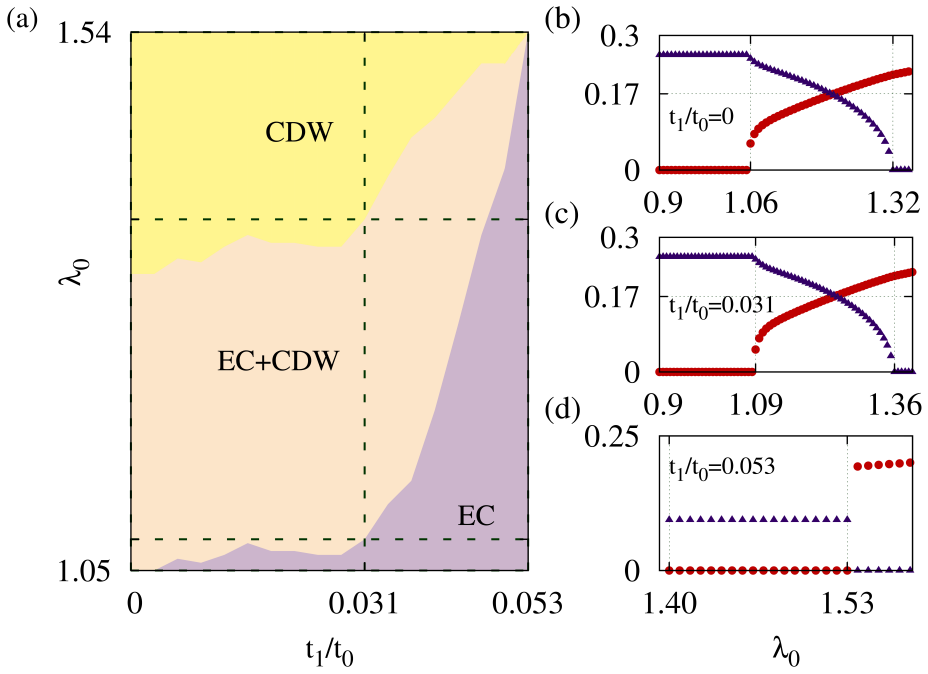

Figure 5.4: Regimes with different coexistence/competition properties are presented for EC and the CDW OPs for varying λ_0 and t_1. Here, increasing t_1 plays the major role in breaking the optimal nesting condition which weakens both OPs, whereas t_1 and λ_0 together determine two regimes of coexistence/competition as indicated in (a). Several cross sections of (a) are given for the EC and CDW order parameters as, b) $t_1 = 0$: EC OP (blue triangles) gradually drops to zero with the onset of CDW (red circles), c) $t_1 = 0.031$: the region of coexistence is narrowed and shifted to higher λ values, and d) $t_1 = 0.053$: a direct transition from EC to CDW, with no coexistence. The OPs on the vertical scale of (b-d) are given in units of t_0.

EC force using Eq.(4.6) which come up to be $\mathcal{F}_{EC} \simeq (1-10) \times 10^{-4} N$ for an area of $A = 10\mu m^2$. In terms of pressure these corresponds to $1Pa$ and $10^7 Pa$ in the close vicinity of the phase boundary respectively. This huge difference of 6 order of magnitude arises due to the large energy scales involved in the TMDC system we are investigating. To give a quantitative demonstration we can use the expression that enables us to write dimensionless pressure that we calculated numerically in units of Pa:

$$\frac{F}{A} = \frac{t_0}{a^3}\eta \ , \qquad \eta = \frac{\Delta\Omega}{t_0}\frac{a^2}{A} \tag{5.32}$$

in which η is the dimensionless change of free energy per area that we calculate numerically. Compared to the system in the previous chapter the length scale

a here is 20 times smaller than a_B and the energy scale t_0 is about 10 times larger than the Hartree energy E_H. Considering this differences in the length and energy scales together with the different values of η, the huge difference of 6 order of magnitude becomes reasonable, and it not only serves our desired goal of obtaining a stronger EC force, which is experimentally more accessible, but it also poses an alternative scenario for the periodic lattice distortions reported in $1T\text{-}TiSe_2$.

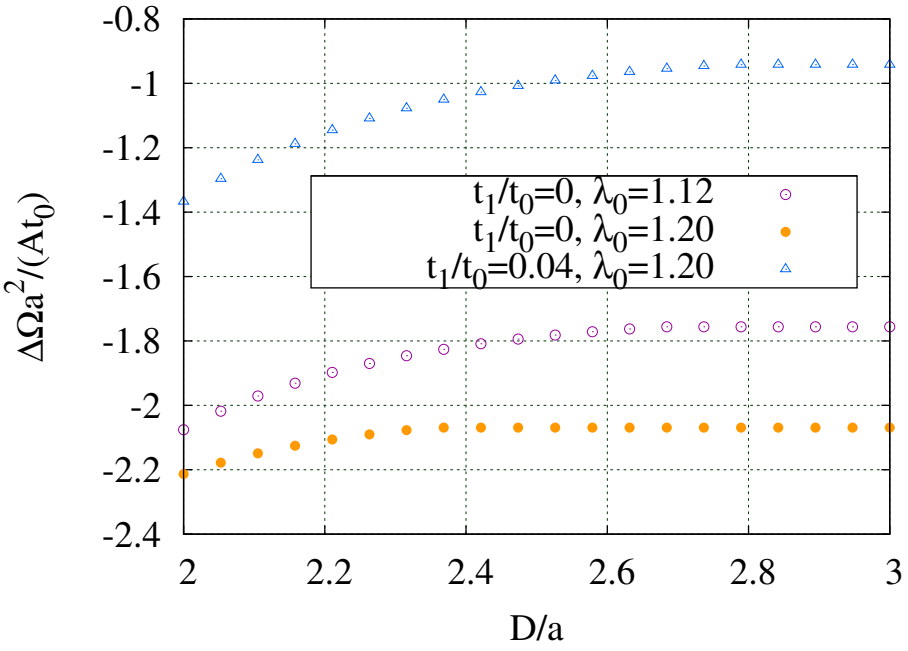

Figure 5.5: The change in the free energy per area with respect to D/a is plotted for different λ_0 and t_1/t_0 values. Free energy becomes constant after EC vanishes, with only CDW remaining, which means that the EC force is zero beyond that critical point.

5.4.3 An Alternative Approach for the Periodic Lattice Distortions in $1T$-$TiSe_2$

Now we can use Eq.(5.31) to estimate the periodic lattice distortions arising in $1T$-$TiSe_2$. Using $a = 5\mathring{A}$ and $E_{Ti} \simeq 100GPa$ [69] for the Young's modulus for the Ti we have $\Delta x_{Ti} \simeq (1-10) \times 10^{-3}\mathring{A}$ which has an order of magnitude agreement with both the experiment[57] and the theoretical calculations[64]. This result justifies the large magnitude we found for the EC-force and moreover it plots an alternative scenario for the periodic lattice distortions observed in $1T$-$TiSe_2$.

5.4.4 Tuning the transition temperatures via electron-phonon interaction

The final result we will demonstrate is the possibility of different configurations of T_c^{EC} and T_c^{CDW}. Fig.(5.6) illustrates all three possibilities, i.e. $T_c^{EC} > T_c^{CDW}$ (Fig.(5.6a)) , $T_c^{EC} = T_c^{CDW}$ (Fig.(5.6b)) and $T_c^{EC} < T_c^{CDW}$ (Fig.(5.6)c,d). This interesting result has an important consequence: Although it is not possible to tune the electron-phonon coupling strength of an individual material, it is always possible to find materials with different electron-phonon coupling strengths. Therefore we can expect to see all three different cases mentioned above.

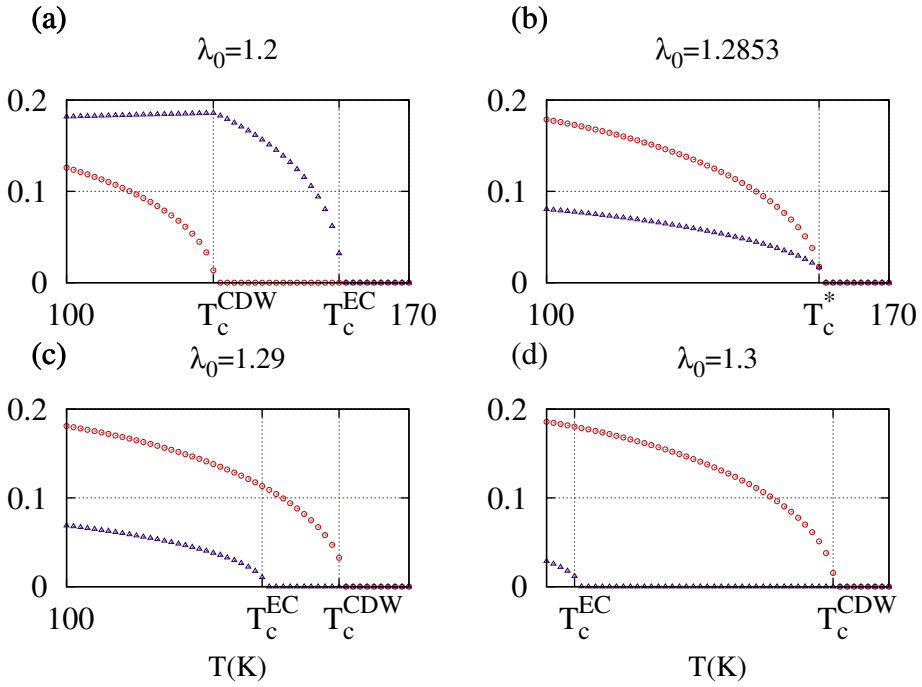

Figure 5.6: Transition temperatures of EC (T_c^{EC}) and CDW (T_c^{CDW}) orders are illustrated for four different λ_0 values for $n_0 \simeq 10^{14} cm^{-2}$ and $t_1 = 0$. a)EC OP has a higher T_c than CDW OP. b) By increasing λ_0 the two critical temperatures were made to coincide at $T = T_c^*$. c) After increasing λ_0 further, CDW order gains a higher T_c. d) Increasing λ_0 even further, the two T_c's can be widely separated. In all four cases, temperature is varied from 100 K to 170 K.

Chapter 6

Conclusion

We demonstrated some exotic features of the EC systems including the robustness against weak magnetic field and emergence of Sarma-I and Sarma-II like phases. We reported a new type of force in condensed matter physics, i.e. EC-force arising in GaAs DQW geometry, due to the presence of the condensate. We also extended the EC formalism of III-V semiconductor systems to the case of layered TMDC, with a focus on $1T$-$TiSe_2$ and posed an alternative scenario for the periodic lattice distortions observed. Once observed, EC-force would give birth to new understandings in condensed matter physics. Moreover, the application of the theory that is described in Chapter 5 to other TMDC materials or layered systems can open new horizons in understanding of various not-yet-fully-understood phenomena. Also the extensions of the theory of competing CDW/EC orders is a promising candidate for contributing to the poorly-understood phenomenon of high temperature superconductivity. The richness of EC systems in physics makes them a perfect candidate for exploring the new frontiers in condensed matter physics.

Bibliography

[1] S. N. Bose, "Plancks gesetz und lichtquantenhypothese" *Z. Phys*, vol. 26, no. 1, pp. 178–181, 1924.

[2] A. Einstein, "Zur theorie der radiometerkrfte" *Zur Theorie der Radiometerkrfte* , vol. 27, no. 1, pp. 1–6, 1924.

[3] S. A. Moskalenko, *Fiz. Tverd. Tela* , vol. 4, pp. 276, 1962.

[4] John M. Blatt, K. W. Ber, and Werner Brandt, "Bose-Einstein Condensation of Excitons" *Phys. Rev.*, vol. 126, no. 5, pp. 1691–1692, 1962.

[5] T. Fukuzawa, E. E. Mendez, and J. M. Hong, "Phase transition of an exciton system in GaAs coupled quantum wells" *Phys. Rev. Lett.*, vol. 64, no. 25, pp. 3066–3069, 1990.

[6] L. V. Butov, A. A. Shashkin, V. T. Dolgopolov, K. L. Campman, and A. C. Gossard, "Magneto-optics of the spatially separated electron and hole layers in $GaAs/Al_xGa_{1x}As$ coupled quantum wells" *Phys. Rev. B*, vol. 60, no. 12, pp. 8753–8758, 1999.

[7] L. V. Butov and A. I. Filin, "Anomalous transport and luminescence of indirect excitons in AlAs/GaAs coupled quantum wells as evidence for exciton condensation" *Phys. Rev. B*, vol. 58, no. 4, pp. 1980–2000, 1998.

[8] A. V. Larionov, V. B. Timofeev, P. A. Ni, S. V. Dubonos, I. Hvam, K. Soerensen , "Bose condensation of interwell excitons in double quantum wells " *JETP*, vol. 75, no. 11, pp. 570–574, 2002.

[9] T. Hakioğlu, E. Özgün "Radiative darkbright instability and the critical Casimir effect in DQW exciton condensates" *Sol. Stat. Com.*, vol. 151, no. 14-15, pp. 1045 – 1048, 2011.

[10] D. W. Snoke "Spontaneous Bose Coherence of Excitons and Polaritons" *Science*, vol. 298, no. 5597, pp. 1368 – 1372, 2002.

[11] T. Hakioğlu and Mehmet ahin "Excitonic Condensation under Spin-Orbit Coupling and BEC-BCS Crossover" *Phys. Rev. Lett.*, vol. 98, no. 16, 166405 2007.

[12] M. Ali Can and T. Hakiolu "Unconventional Pairing in Excitonic Condensates under Spin-Orbit Coupling" *Phys. Rev. Lett.*, vol. 103, no. 8, 086404, 2009.

[13] M. Kellogg, J. P. Eisenstein, L. N. Pfeiffer, K. W. West "Evidence for $2k_F$ electronelectron scattering processes in Coulomb drag" *Sol. Stat. Comm.*, vol. 123, no. 12, pp. 515 – 519, 2002.

[14] M. P. Lilly, J. P. Eisenstein, L. N. Pfeiffer, and K. W. West "Coulomb Drag in the Extreme Quantum Limit" *Phys. Rev. Lett.*, vol. 80, no. 8, pp. 1714 – 1717, 1998.

[15] M. Kellogg, J. P. Eisenstein, L. N. Pfeiffer, and K. W. West "Bilayer Quantum Hall Systems at $\nu_T = 1$: Coulomb Drag and the Transition from Weak to Strong Interlayer Coupling" *Phys. Rev. Lett.*, vol. 90, no. 24, 2003.

[16] T. J. Gramila, J. P. Eisenstein, A. H. MacDonald, L. N. Pfeiffer, and K. W. West "Mutual friction between parallel two-dimensional electron systems" *Phys. Rev. Lett.*, vol. 66, no. 9, pp. 1216 – 1219, 1991.

[17] M. Kellogg, I. B. Spielman, J. P. Eisenstein, L. N. Pfeiffer, and K. W. West "Observation of Quantized Hall Drag in a Strongly Correlated Bilayer Electron System" *Phys. Rev. Lett.*, vol. 88, no. 12, 2002.

[18] T. Hakioğlu, E. Özgün, M. Günay "A measurable force driven by an excitonic condensate" *Appl. Phys. Let.*, vol. 104, no. 16, 2014.

[19] A. A. High, J. R. Leonard, A. T. Hammack, M. M. Fogler, L. V. Butov, A. V. Kavokin K. L. Campman and A. C. Gossard "Spontaneous coherence in a cold exciton gas" *Nature*, vol. 483, no. 7391, pp. 584 – 588, 2012.

[20] J. Frenkel "On the Transformation of light into Heat in Solids. I" *Phys. Rev.*, vol. 37, no. 1, pp. 17 – 44, 1931.

[21] G. H. Wannier "The Structure of Electronic Excitation Levels in Insulating Crystals" *Phys. Rev.*, vol. 52, no. 3, pp. 191 – 197, 1937.

[22] N. F. Mott "Conduction in polar crystals. II. The conduction band and ultra-violet absorption of alkali-halide crystals " *Trans. Faraday Soc.*, vol. 34, pp. 500 – 506, 1938.

[23] M. Tinkham, "Group Theory and Quantum Mechanics" *Dover*, New York, USA, 2003.

[24] S. A. Moskalenko, D. W. Snoke "Bose-Einstein Condensation of Excitons and Biexcitons," *Cambridge University Press*, New York, USA, 2000.

[25] Monique Combescot, O. Betbeder-Matibet, Roland Combescot, "Bose-Einstein Condensation in Semiconductors: The Key Role of Dark Excitons" *Phys. Rev. Lett.*, vol. 99, no. 17, 176403, 2007.

[26] M.Combescot,O.Betbeder-Matibet, "Coherent effects in the physics of composite excitons" *Phys. Rev. B*, vol. 74, no. 4, 045110, 2006.

[27] H. Bruus, K. Flensberg "Many-Body Quantum Theory in Condensed Matter Physics" *Oxford*, New York, USA, 2004.

[28] M. Sigrist, K. Ueda "Phenomenological theory of unconventional superconductivity" *Rev. Mod. Phys.*, vol. 63, no. 2, pp. 239 – 311, 1991.

[29] J. Bardeen, L. N. Cooper, J. R. Schrieffer "Theory of Superconductivity" *Phys. Rev.*, vol.108, no.5, pp. 1175 – 1204, 1957.

[30] T. Hakioğlu, E. Özgün, M. Günay "Robust ground state and artificial gauge in DQW exciton condensates under weak magnetic field" *Physica E*, vol. 62, pp. 10 – 14, 2014.

[31] G. Sarma "On the influence of a uniform exchange field acting on the spins of the conduction electrons in a superconductor" *J. Phys. Chem. Solids*, vol. 24, no. 8, pp. 1029 – 1032, 1963.

[32] P. Pieri, D. Neilson, G. C. Strinati "Effects of density imbalance on the BCS-BEC crossover in semiconductor electron-hole bilayers" *Phys. Rev. B*, vol. 75, no. 11, 2007.

[33] Lianyi He, Meng Jin, Pengfei Zhuang "LOFF pairing vs breached pairing in asymmetric fermion superfluids" *Phys. Rev. B*, vol. 73, no. 21, 2006.

[34] K. B. Gubbels, M. W. J. Romans, H. T. C. Stoof "On the influence of a uniform exchange field acting on the spins of the conduction electrons in a superconductor" *Phys. Rev. Let*, vol. 97, no. 21, 2006.

[35] Yan He, Chih-Chun Chien, Qijin Chen, K. Levin "Single-plane-wave Larkin-Ovchinnikov-Fulde-Ferrell state in BCS-BEC crossover" *Phys. Rev. A*, vol. 75, no. 2, 2007.

[36] Michael McNeil Forbes, Elena Gubankova, W. Vincent Liu, Frank Wilczek "Stability Criteria for Breached-Pair Superfluidity" *Phys. Rev. Let.*, vol. 94, no. 1, 2005.

[37] M. J. Snelling, E. Blackwood, C. J. McDonagh, R. T. Harley, and C. T. B. Foxona "Exciton, heavy-hole, and electron g factors in type-I $GaAs/Al_xGa_{1x}As$ quantum wells" *Phys. Rev. B*, vol. 45, no. 7, pp. 3922 – 3925, 1992.

[38] R. Winkler, " SpinOrbit Coupling Effects in Two-Dimensional Electronand Hole Systems," *Springer* Berlin ,Germany, 2003.

[39] H. B. G. Casimir "On the attraction between two perfectly conducting plates" *Proc. K. Ned. Akad. Wet.*, vol. 51, no. 793, pp. 150, 1948.

[40] M. E. Fisher and P. G. de Gennes "Wall phenomena in a critical binary mixture" *C.R. Acad. Sci, Paris Ser B*, vol. 287, no. 8-15, pp. 207 – 09, 1978.

[41] C. Hertlein, L. Helden, A. Gambassi S. Dietrich and C. Bechinger "Direct measurement of critical Casimir forces" *Nature*, vol. 451, no. 7175, pp. 172 – 175, 2008.

[42] Masafumi Fukuto, Yohko F. Yano, and Peter S. Pershan "Critical Casimir Effect in Three-Dimensional Ising Systems: Measurements on Binary Wetting Films" *Phys. Rev. Lett.*, vol. 94, no. 13, 2005.

[43] R. Garcia and M. H. W. Chan "Critical Casimir Effect near the ^3He–^4He Tricritical Point" *Phys. Rev. Lett.*, vol. 88, no. 8, 2002.

[44] S. Biswas, J. K. Bhattacharjee, H. S. Samanta, S. Bhattacharyya and B. Hu, "The critical Casimir force in the superfluid phase: effect of fluctuations" *N. Jour. Phys.*, vol. 12, no. 6, 2010.

[45] P. A. Martin and V. A. Zagrebnov "The Casimir effect for the Bose-gas in slabs" *Europhys. Lett.*, vol. 73, no. 1,2006.

[46] J. M. Obrecht, R. J. Wild, M. Antezza, L. P. Pitaevskii, S. Stringari, and E. A. Cornell "Measurement of the Temperature Dependence of the Casimir-Polder Force" *Phys. Rev. Lett.*, vol. 98, no. 6, 2007.

[47] D. M. Harber, J. M. Obrecht, J. M. McGuirk, and E. A. Cornell "Measurement of the Casimir-Polder force through center-of-mass oscillations of a Bose-Einstein condensate" *Phys. Rev. A*, vol. 72, no. 3, 2005.

[48] L. V. Butov "Condensation and pattern formation in cold exciton gases in coupled quantum wells" *J.Phys.: Cond. Mat.*, vol. 16, no. 50, 2004.

[49] L. V. Butov"Cold exciton gases in coupled quantum well structures" *J.Phys.: Cond. Mat.*, vol. 19, no. 29, 2007.

[50] Walter Greiner, Ludwig Neise, Horst Stcke "Thermodynamics and Statistical Mechanics", *Springer*, USA, 1995.

[51] K. Levin, D. L. Mills, and S. L. Cunningham "Incompatibility of BCS pairing and the Peierls distortion in one-dimensional systems. I. Mean-field theory" *Phys. Rev. B*, vol. 10, no. 9, pp. 3821 – 3831, 1974.

[52] Griff Bilbro and W. L. McMillan "Theoretical model of superconductivity and the martensitic transformation in A15 compounds" *Phys. Rev. B*, vol. 14, no. 5, pp. 1887 – 1892, 1976.

[53] C. A. Balseiro, L. M. Falicov "Superconductivity and charge-density waves" *Phys. Rev. B*, vol. 20, no. 11, pp. 4457 – 4464, 1979.

[54] J. A. Wilson, A. D. Yoffe "The transition metal dichalcogenides discussion and interpretation of the observed optical, electrical and structural properties" *Adv. Phys.*, vol. 18, no. 73, pp. 193 – 335, 1969.

[55] A. M. Gabovich, A. I. Voitenko, M. Ausloos "Charge- and spin-density waves in existing superconductors: competition between Cooper pairing and Peierls or excitonic instabilities" *Phys. Rep.*, vol. 367, no. 6, pp. 583 – 709, 2002.

[56] K. C. Woo, F. C. Brown, W. L. McMillan, R. J. Miller, M. J. Schaffman, and M. P. Sears "Superlattice formation in titanium diselenide" *Phys. Rev. B*, vol. 14, no. 8, pp. 3242 – 3247, 1976.

[57] F. J. Di Salvo, D. E. Moncton, and J. V. Waszczak "Electronic properties and superlattice formation in the semimetal $TiSe_2$" *Phys. Rev. B*, vol. 14, no. 10, pp. 4321 – 4328, 1976.

[58] N. Suzuki, A. Yamamoto, K. Motizuki "Electron-lattice interaction and the CDW state of 1T-$TiSe_2$" *Sol. Stat. Comm.*, vol. 49, no. 11, pp. 1039 – 1043, 1984.

[59] Th. Pillo, J. Hayoz, H. Berger, F. Lvy, L. Schlapbach, and P. Aebi "Photoemission of bands above the Fermi level: The excitonic insulator phase transition in 1T-$TiSe_2$" *Phys. Rev. B*, vol. 61, no. 23, pp. 16213 – 16222, 2000.

[60] K. Rossnagel, L. Kipp, and M. Skibowski "Charge-density-wave phase transition in 1T-$TiSe_2$: Excitonic insulator versus band-type Jahn-Teller mechanism" *Phys. Rev. B*, vol. 65, no. 23, 2002.

[61] T. E. Kidd, T. Miller, M. Y. Chou, and T. -C. Chiang "Electron-Hole Coupling and the Charge Density Wave Transition in $1T$-$TiSe_2$" *Phys. Rev. Lett.*, vol. 88, no. 22, 2002.

[62] H. Cercellier, C. Monney, F. Clerc, C. Battaglia, L. Despont, M. G. Garnier, H. Beck, P. Aebi, L. Patthey, H. Berger, and L. Forr "Evidence for an Excitonic Insulator Phase in $1T$-$TiSe_2$" *Phys. Rev. Lett.*, vol. 99, no. 14, 2007.

[63] C. Monney, H. Cercellier, F. Clerc, C. Battaglia, E. F. Schwier, C. Didiot, M. G. Garnier, H. Beck, P. Aebi, H. Berger, L. Forr, and L. Patthey "Spontaneous exciton condensation in $1T$-$TiSe_2$: BCS-like approach" *Phys. Rev. B*, vol. 79, no. 4, 2009.

[64] C. Monney, C. Battaglia, H. Cercellier, P. Aebi, and H. Beck "Exciton Condensation Driving the Periodic Lattice Distortion of $1T$-$TiSe_2$" *Phys. Rev. Lett.*, vol. 106, no. 10, 2011.

[65] E. Özgün and T. Hakioğlu, "CDW-Exciton condensate competition and a condensate driven force" *Europhys. Lett.* (submitted)

[66] George Grüner, "Density Waves in Solids", *Perseus Publishing*, Boston, USA, 1994.

[67] Bogdan Mihaila, "Lindhard function of a d-dimensional Fermi gas" *Preprint*, arXiv:1111.5337v1, 2011.

[68] H. Fröhlich, "Electrons in lattice fields " *Adv. Phys.*, vol. 3, no. 11, pp. 325 – 361, 1954.

[69] "The selection and use of Titanium: A design guide", *Institute of materials*, Great Britain, 1995.

Appendix A

Code

```
parameter (mx=50)
parameter (my=50)
double precision pi, qnx, qny, T, beta, e_scale, tol, xlam, D
double precision t0, t1, cp, deb, qx(mx), wx(mx), qy(my), wy(my)
double precision G0, G1, del(mx,my), kx, ky, sum1x, sum2x, sum3x
double precision sum1y(mx), sum2y(mx), sum3y(mx), G, epsk, epskq
double precision epsp, epsm, kpx, kpy, E0, E1, E2, fd1, fd2, lm
double precision sing, cnt1, temp1, temp2, temp3(mx,my), xcut
double precision aux, f, temp4, bigK, temp5, temp6, temp7(mx,my)
double precision cntrl, comp, free, term1, term2, term3, term4
double precision E1p, E2p, fd1p, fd2p, sum4x, sum5x, sum6x
double precision sum4y(mx), sum5y(mx), sum6y(mx), dstep, dfree
double precision temp_free, fpa, sum7x, sum7y(mx), density
double precision sum8x, sum8y(mx), temp8, tempG, dfd1, dfd2
double precision D_adapt
integer istep, icnt
external gauleg
intrinsic datan,dexp, dsqrt, dcos, dabs, dcosh
open(1,file='data/cp38.dat')
```

```
open(2,file='data/tc42.dat')
open(3,file='data/na38.dat')
open(4,file='data/disp36.dat')
pi = 4d0*datan(1d0)
qnx = pi
qny = pi
!-----------------------------------------------------------------------
density = 0.499
xcut = 1d-10
cntrl = 1d-4
dstep = 0.0001
istep = 500000
tol = 1d-8
e_scale = 0.125
bigK = 0.
do ijk=1,101
T =  165. - (ijk-1.)
temp_free = 0.
dfree = 0.
fpa = 0.
do jj=1,2
D = 2.05 + dstep*(jj-1)
t0 = 1.
do jjj=1,1
t1 = 0.
do ii=1,1
temp4 = 0.
icnt = 0
xlam = 1.2853 +(ii-1)/39.*0.45   !1.2
!-----------------------------------------------------------------------
beta = e_scale/(8.617*T)*1d5
deb = 1./3.
call gauleg(-pi,pi,qx,wx,mx)
```

```
call gauleg(-pi,pi,qy,wy,my)
if(jj.eq.1.and.ii.eq.1.and.ijk.eq.1.or.G.le.cntrl) then
G0 = 0.1
G1 = 0.1
cp = 0.
endif
if(jj.eq.1.and.ii.eq.1.and.ijk.eq.1) then
do i=1,mx
    do j=1,my
        del(i,j) = 1d-1*dexp(-1d-1*(qx(i)*qx(i)+qy(j)*qy(j)))
    enddo
enddo
endif
!-----------------------------------------------------------------------
      DO it=1,istep
      cnt1 = 0
      temp9 = cp
 66   sum1x = 0.
      sum2x = 0.
      sum7x = 0.
      sum8x = 0.
      do i=1,mx
      kx = qx(i)
      sum1y(i) = 0.
      sum2y(i) = 0.
      sum7y(i) = 0.
      sum8y(i) = 0.
      do j=1,my
          ky = qy(j)
          epsk = -2.*t0*(dcos(kx)+dcos(ky))-
     2             4.*t1*(dcos(kx)*dcos(ky))
          epskq = -2.*t0*(dcos(kx+qnx)+dcos(ky+qny))-
     2              4.*t1*(dcos(kx+qnx)*dcos(ky+qny))
```

```
epsp = (epsk+epskq)/2.
epsm = (epsk-epskq)/2.
G = G0
if(dabs(epsk-cp).lt.deb) then
G = G0+G1
endif
lm = dsqrt(epsm**2.+G*G+del(i,j)**2.)
E0 = epsp-cp
E1 = E0+lm
E2 = E0-lm
fd1 = 1./(1.+dexp(beta*E1))
fd2 = 1./(1.+dexp(beta*E2))
dfd1 = beta/(4.*dcosh(beta*E1/2.)*dcosh(beta*E1/2.))
dfd2 = beta/(4.*dcosh(beta*E2/2.)*dcosh(beta*E2/2.))
if(beta*E1.lt.-15d0) then
fd1 = 1.
endif
if(beta*E1.gt.15d0) then
fd1 = 0.
endif
if(beta*E2.lt.-15d0) then
fd2 = 1.
endif
if(beta*E2.gt.15d0) then
fd2 = 0.
endif
sum1y(i) = sum1y(i)
sum2y(i) = sum2y(i)+wy(j)*G*(fd1-fd2)/(2.*lm)
if(dabs(epsk-cp).lt.deb.and.dabs(epskq-cp).lt.deb) then
sum1y(i) = sum1y(i)+wy(j)*(fd1-fd2)/(2.*lm)
endif
f = del(i,j)*(fd1-fd2)/(2.*lm)
sum7y(i) = sum7y(i) +wy(j)*
```

```
     2                ((lm+epsm)/lm*fd1+(lm-epsm)/lm*fd2)
          sum8y(i) = sum8y(i) +wy(j)*
     2                ((lm+epsm)/lm*dfd1+(lm-epsm)/lm*dfd2)
          tempG = G0 + G1
!//////--------/////////---------/////////--------
          sum3x = 0.
          do ip=1,mx
               kpx = qx(ip)
               sum3y(ip) = 0.
               do jp=1,my
                    kpy = qy(jp)
                    epsk = -2.*t0*(dcos(kpx)+dcos(kpy))-
     2                      4.*t1*(dcos(kpx)*dcos(kpy))
                    epskq = -2.*t0*(dcos(kpx+qnx)+dcos(kpy+qny))-
     2                       4.*t1*(dcos(kpx+qnx)*dcos(kpy+qny))
                    epsp = (epsk+epskq)/2.
                    epsm = (epsk-epskq)/2.
                    G = G0
                    if(dabs(epsk-cp).lt.deb) then
                    G = G0+G1
                    endif
                    lm = dsqrt(epsm**2.+G*G+del(ip,jp)**2.)
                    E0 = epsp-cp
                    E1 = E0+lm
                    E2 = E0-lm
                    fd1 = 1./(1.+dexp(beta*E1))
                    fd2 = 1./(1.+dexp(beta*E2))
                    if(beta*E1.lt.-15d0) then
                    fd1 = 1.
                    endif
                    if(beta*E1.gt.15d0) then
                    fd1 = 0.
                    endif
```

```
                if(beta*E2.lt.-15d0) then
                fd2 = 1.
                endif
                if(beta*E2.gt.15d0) then
                fd2 = 0.
                endif
                sing = dsqrt((kx-kpx)**2.+(ky-kpy)**2.)
                aux = dexp(-sing*D)/(sing)
                if(dabs(sing).lt.dsqrt(xcut)) then
                aux = 0.
                endif
                sum3y(ip) = sum3y(ip)+wy(jp)*aux*
     2                (del(ip,jp)*(fd1-fd2)/(2.*lm)-f)
              enddo
              sum3x = sum3x+wx(ip)*sum3y(ip)
            enddo
            temp3(i,j) = -0.5*15./(4.*pi*pi)*(sum3x+(2.*pi/D)*f)
          enddo
          sum1x = sum1x+wx(i)*sum1y(i)
          sum2x = sum2x+wx(i)*sum2y(i)
          sum7x = sum7x+wx(i)*sum7y(i)
          sum8x = sum8x+wx(i)*sum8y(i)
          enddo
          temp1 = -xlam*sum1x*(tempG)/(4.*pi*pi)
          temp2 = -xlam*sum2x/(4.*pi*pi)
          temp8 = cp - (density-sum7x/(2.*(2.*pi)**2.))/
     2                (-sum8x/(2.*(2.*pi)**2.))
          if(dabs(density-sum7x/(2.*(2.*pi)**2.)).gt.tol) then
          cp = temp8
          goto 66
          endif
          cp = temp9
          if(dabs(G0-temp1).lt.tol.and.dabs(G1-temp2).lt.tol
```

```
     2                                   .and.dabs(cp-temp8).lt.tol) then
      cnt1 = 3
      endif
      do i=1,mx
           do j=1,my
           if(dabs(del(i,j)-temp3(i,j)).lt.tol) then
           cnt1 = cnt1 + 1
           endif
           enddo
      enddo
      if(cnt1.eq.mx*my+3) then
      icnt = it
      goto 88
      endif
      G0 = temp1
      G1 = temp2
      cp = temp8
      do i=1,mx
           do j=1,my
                del(i,j) = temp3(i,j)
           enddo
      enddo
     ENDDO ! iteration ends
 88   G0 = temp1
      G1 = temp2
      cp = temp8
      do i=1,mx
           do j=1,my
                del(i,j) = temp3(i,j)
                if(del(i,j).gt.temp4) then
                bigK = del(i,j)
                temp4= del(i,j)
                endif
```

```
        write(1,100) qx(i), qy(j), G0+G1, del(i,j), cp, D, T ,t1,icnt
        call flush(1)
            enddo
        enddo
        comp = datan(bigK/(G0+G1))
        write(2,200) G0+G1, bigK, comp, cp, D, T, xlam, icnt
!!!!!!!!!!!!!!!!!!!!!!!!!!!!FREE ENERGY!!!!!!!!!!!!!!!!!!!!!!!!!!
free = 0.
sum4x = 0.
sum5x = 0.
sum6x = 0.
do i=1,mx
    kx=qx(i)
    sum4y(i) = 0.
    sum5y(i) = 0.
    sum6y(i) = 0.
    do j=1,my
        ky=qy(j)
        epsk = -2.*t0*(dcos(kx)+dcos(ky))-
   2                4.*t1*(dcos(kx)*dcos(ky))
        epskq = -2.*t0*(dcos(kx+qnx)+dcos(ky+qny))-
   2                4.*t1*(dcos(kx+qnx)*dcos(ky+qny))
        epsp = (epsk+epskq)/2.
        epsm = (epsk-epskq)/2.
        G = G0
        if(dabs(epsk-cp).lt.deb) then
        G = G0+G1
        endif
        lm = dsqrt(epsm**2.+G*G+del(i,j)**2.)
        E0 = epsp-cp
        E1 = E0+lm
        E2 = E0-lm
        E1p = E0+epsm
```

```
      E2p = E0-epsm
      fd1 = 1./(1.+dexp(beta*E1))
      fd2 = 1./(1.+dexp(beta*E2))
      fd1p = 1./(1.+dexp(beta*E1p))
      fd2p = 1./(1.+dexp(beta*E2p))
      if(beta*E1.lt.-15d0) then
      fd1 = 1.
      endif
      if(beta*E1.gt.15d0) then
      fd1 = 0.
      endif
      if(beta*E2.lt.-15d0) then
      fd2 = 1.
      endif
      if(beta*E2.gt.15d0) then
      fd2 = 0.
      endif
      if(beta*E1p.lt.-15d0) then
      fd1p = 1.
      endif
      if(beta*E1p.gt.15d0) then
      fd1p = 0.
      endif
      if(beta*E2p.lt.-15d0) then
      fd2p = 1.
      endif
      if(beta*E2p.gt.15d0) then
      fd2p = 0.
      endif
      sum4y(i) = sum4y(i)+wy(j)*del(i,j)**2./(2.*lm)*(fd1-fd2)
      sum5y(i) = sum5y(i)+wy(j)*(E1*fd1+E2*fd2)
      sum6y(i) = sum6y(i)+wy(j)*(E1p*fd1p+E2p*fd2p)
enddo
```

```
      sum4x = sum4x +wx(i)*sum4y(i)
      sum5x = sum5x +wx(i)*sum5y(i)
      sum6x = sum6x +wx(i)*sum6y(i)
    enddo
    term1 = -G0*G1/xlam
    term2 = sum4x
    term3 = 2.*sum5x
    term4 = -2.*sum6x
    free = term1+term2+term3+term4
!!!!!!!!!!!!!!!!!!!!!!!!!!!!!!!!!!!!!!!!!!!!!!!!!!!!!!!!!!!!!!!!!!!!!!!!!!!!!!!
          write(3,300) term1,term2,term3,term4,free,D,xlam,t1,icnt
          call flush(3)
          if (ii.eq.1) then
          temp5 = G0
          temp6 = G1
          do i=1,mx
               do j=1,my
                    temp7(i,j) = del(i,j)
               enddo
          enddo
          endif
          enddo   !xlam
          G0 = temp5
          G1 = temp6
          do i=1,mx
               do j=1,my
                    del(i,j) = temp7(i,j)
               enddo
          enddo
          enddo   !t1
!use only to calculate temperature dependent force
          if(jj.eq.1) then
          temp_free = free
```

```
      endif
      enddo   !D
      dfree = free-temp_free
      fpa = dfree/dstep
      write(4,400) fpa,T,D,dfree,xlam,icnt
      call flush(4)
      enddo !T
100   format(3(f12.7,2x),f20.12,2x,4(f12.7,2x),i5)
200   format(f12.7,2x,f20.12,2x,5(f12.7,2x),i5)
300   format(8(f12.7,2x),i5)
400   format(3(f12.7,2x),f20.12,2x,f12.7,2x,i5)
      end
```